

UNCLASSIFIED

AD NUMBER

AD861884

LIMITATION CHANGES

TO:

Approved for public release; distribution is unlimited.

FROM:

Distribution authorized to DoD only;
Proprietary Information; 17 OCT 1969. Other
requests shall be referred to U.S. Naval
Weapons Laboratory, Dahlgren, VA.

AUTHORITY

USNWL ltr, 24 May 1972

THIS PAGE IS UNCLASSIFIED

L

AD861884

DDC FILE COPY

25

F70

TECHNICAL REPORT

AN EXPERIMENTAL INVESTIGATION OF THE EFFECTS OF A BLAST WAVE ON A VEHICLE IN A SUPERSONIC FLOW

By: R. P. Mason

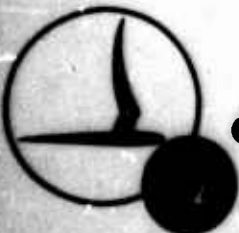
CAL No. GM-2673-D-4

Prepared for:

UNITED STATES NAVAL WEAPONS LABORATORY
DAHLGREN, VIRGINIA

Contract No. N00178-69-C-0013
17 OCTOBER 1969

Handwritten signatures and initials.



CORNELL AERONAUTICAL LABORATORY, INC.

OF CORNELL UNIVERSITY, BUFFALO, N. Y. 14221

770



CORNELL AERONAUTICAL LABORATORY, INC.
BUFFALO, NEW YORK 14221

(14) CAL  GM-2673-D-4

(9) Technical rept.,

(6) AN EXPERIMENTAL INVESTIGATION OF THE
EFFECTS OF A BLAST WAVE ON A VEHICLE
IN A SUPERSONIC FLOW.

D D C

NOV 26 1969

(10) R. Paul / Mason

(15) CONTRACT NO.  178-68-C-8313

(11) 17 OCT 

(12) 89p.

Each transmittal of this document outside the Department of Defense must have prior approval of the Technical Library, U. S. Naval Weapons Laboratory, Dahlgren, Virginia 22448.

(16) ORD-622-214/09421/UF20-352-503

Prepared For:

UNITED STATES NAVAL WEAPONS LABORATORY
DAHLGREN, VIRGINIA

PREPARED BY: R. Paul Mason

R.P. Mason
Hypersonic Facilities Dept.

APPROVED BY: J.F. Martin

J.F. Martin, Head
Hypersonic Facilities Dept.

REVIEWED BY: Thomas W. Egan

Thomas W. Egan
ATV Project Engineer
Weapons Research Dept.

098 300

mt

FOREWORD

This report was prepared by the Cornell Aeronautical Laboratory (CAL), Buffalo, New York, under Navy contract N00178-68-C-0313. This effort is part of an Aerial Target Vulnerability (ATV) study being conducted by the Naval Weapons Laboratory (NWL), Dahlgren, Virginia, under NAVORD-SYSCOMHQORDTASK ORD-622-214/0901/UF20-352-503.

The principal author was Mr. R. Paul Mason of the Hypersonic Facilities Department. The NWL program manager was Mr. W. W. Morton of the Systems Analysis Division-Surface Warfare Department.

The objective of the Aerial Target Vulnerability program is to delineate the vulnerability of selected potential foreign aerial targets to the terminal damage mechanisms of conventional anti-air guided missile ordnance. This is an applied research effort which is being conducted expressly in support of the Navy's anti-air guided missile ordnance development and evaluation efforts.

Data from the blast tests reported herein will be correlated with a concurrent CAL analytical blast damage analysis. The resulting information will be used by NWL in evaluating the blast effects of various type warheads on the vulnerability of aerial targets.

Systems Analysis Division
Surface Warfare Department
U. S. Naval Weapons Laboratory

ACKNOWLEDGEMENTS

The work reported herein was performed by various CAL personnel assigned to this program. In particular, major contributions to the technical effort were made by the following:

L. Bogdan	Instrumentation Development
R. P. Mason	Test Engineer

In addition, assistance has been provided to CAL in the collection of the data contained herein by several individuals and organizations within the Department of Defense. In particular, acknowledgement is made to the following contributors:

W. W. Morton	Program Manager, U. S. Naval Weapons Laboratory, Dahlgren, Virginia
S. R. Garrison	U. S. Naval Weapons Laboratory, Dahlgren, Virginia

SUMMARY

A test was conducted at Cornell Aeronautical Laboratory (CAL) to determine the effects of a blast wave on a delta-wing model in a supersonic flow ($M \approx 2.0$). Pressure data were taken at various locations on the model using fast-response pressure transducers.

The blast wave was generated by the detonation of a small explosive charge at the apex of a hollow cone normal to the flow direction. The variables of the test were model attitude relative to the charge and simulated altitude.

This report presents details of the facility, blast generator and model, describes the development of instrumentation, presents the results of the tests and explicit conclusions and recommendations.

LIST OF TABLES

1. Run Schedule (Static Cone Calibrations)
2. Performance of Conical Shock Tubes
3. Run Schedule (Model Data Runs)

LIST OF ILLUSTRATIONS

1. General Arrangement of the External Flow System as Modified for Blast Wave Tests
2. Blast Cone Photograph
3. Schematic of Explosive Train
4. Model Installation
5. Model Installation Photograph
6. Pitot Survey Rake Installation Photograph
7. Blast Generator Instrumentation Locations
8. Transducer Mounting Techniques
9. Typical Transducer Installation, Showing Miniature Source Follower Circuit
10. Model Instrumentation Locations
11. Schematic of Flow Visualization System
12. Oscilloscope Records from a Static, Cone Calibration Run
13. Cone Calibration Data
 - (a) Incident Overpressure as a Function of Scaled Distance
 - (b) Reflected Overpressure as a Function of Scaled Distance
14. Shock Time-of-Arrival as a Function of Charge Weight
15. Shadowgraph Photograph of Cone-Calibration Flat Plate
16. Nozzle Pitot Pressure Profile
17. Schlieren Photograph of Pitot Survey Rake
18. Selected Oscilloscope Records for a Model Run with Supersonic Flow and a Blast Wave
19. Peak Overpressure on Model as a Function of Roll Angle
20. Peak Overpressure as a Function of Simulated Altitude
21. Peak Overpressure as a Function of Charge Weight
22. Shadowgraph Photograph of the Model in Supersonic Flows with Blast Wave

NOMENCLATURE AND SYMBOLS

Kft	Thousands of feet (altitude)
M	Mach No.
P_o	Ambient pressure, atmospheres
P_R	Reflected overpressure (psi); (pressure behind reflected wave) - (ambient pressure)
P_s	Incident overpressure (psi); (pressure behind incident wave) - (ambient pressure)
P_t	Total or reservoir pressure (psi)
P_o'	Pitot pressure in test section (psi) - total pressure behind normal shock
R	Distance from charge, ft
t	Time of arrival of shock, measured from charge initiation (msec.)
W	Charge weight (lbs. wt.)
Z	Scaled distance ($R/W^{1/3}$)
Z'	Scaled distance with altitude scaling $\frac{P_o^{1/3} \cdot R}{W^{1/3}}$
α	Model angle of attack (nose up positive)
ϕ	Model angle of roll (right wing down positive)

TABLE OF CONTENTS

<u>Section</u>		<u>Page</u>
	FOREWORD	i
	ACKNOWLEDGEMENTS	ii
	SUMMARY	iii
	LIST OF TABLES	iv
	LIST OF ILLUSTRATIONS	v
	NOMENCLATURE AND SYMBOLS	vi
I.	INTRODUCTION	1
II.	TEST EQUIPMENT	3
	A. External Flow System	3
	B. Blast Cone and Nozzle Extension	3
	C. Explosive and Initiators	4
	D. Model and Model Support	4
	E. Airflow Rake	5
	F. Instrumentation and Data Recording	5
	G. Flow Visualization	6
III.	TEST PROCEDURE	8
	A. Calibration of Pressure Transducers	8
	B. Test Program	8
	C. Test Operation	9
IV.	DATA REDUCTION	11
V.	PRESENTATION OF DATA	12
	A. Cone Calibration	12
	B. Nozzle Airflow	13
	C. Model Data	13
	D. Limitations of the Experimental Technique	16

<u>Section</u>		<u>Page</u>
VI.	PRECISION OF DATA	18
VII.	CONCLUSIONS AND RECOMMENDATIONS	19
	REFERENCES	21
	TABLES	
	ILLUSTRATIONS	
	APPENDIX A	
	APPENDIX B	

I. INTRODUCTION

In the past, many investigations of the effects of a blast wave on a body in supersonic and hypersonic flows have been undertaken. These, however, have usually been restricted to optical investigations of the blast-shock interaction (pressure data rarely being taken) on simple shapes such as spheres, cones, and wedges. Further, they have usually employed blast-wave generators, such as shock tubes, which have provided the essentially planar shocks typical of nuclear explosions.

On the other hand, investigators concerned with the local blast effects on structures due to nonnuclear explosions have simulated these by means of high energy conventional explosives, sometimes amplified by using a hollow cone with the explosives in the apex.

There remained a gap in existing experimental techniques in that the effects of nearby conventional explosions on typical aircraft could not be assessed at different vehicle velocities, attitudes, and altitudes. The purpose of the reported tests was to demonstrate the feasibility of an experimental technique to determine these effects and to obtain some preliminary data on a simple model.

The reported tests will be correlated with the analytical blast damage investigation being conducted by CAL under this contract. These two project tasks are intended to assist the overall NWL ATV program in assessing the vulnerability of aerial targets to both blast-only warheads and other types of warheads where blast enhancement of the primary kill mechanism is obtained.

The technique uses a blow-down type supersonic wind tunnel which operates on an unsteady flow principle. The run time, although short, is sufficient to establish steady flow over the model. Synchronized with the flow, a conical blast generator provides a blast wave normal to the flow direction which passes through the flow field around the model and then intercepts the model. Because of the nature of the pressure time history due to the blast wave, it was necessary to give considerable care to the selection and use of pressure transducers and electric filters.

The tests reported herein were conducted in the External Flow System of the Hypersonic Facilities Department during the period 27 May 1969 to 25 June 1969. The External Flow System is the property of the National Aeronautics and Space Administration, accountable under NASA Facilities Contract No. NAS8-20878 (F) and was made available for this program by their permission.

The model, data, and photographs are UNCLASSIFIED.

II. TEST EQUIPMENT

A. External Flow System

The short-duration external-flow system is basically a blow-down wind tunnel which operates according to the nonsteady flow principles discussed in References 1 and 2. The dry* test air is initially contained in a high-pressure supply tube by a plastic diaphragm. Mechanical cutting of this diaphragm allows the air to exhaust through a nozzle and into a vacuum chamber. The nozzle exit flow Mach number is about 2. For the 30-foot-long supply tube currently used, a steady nozzle supply is maintained for about 40 msec. when using room temperature air as the test gas. The facility was originally constructed for base heating tests (e. g., Reference 3) and included a centerbody which was terminated at a point just upstream of the throat for the reported test.

The system, as modified for the test, is shown in Figure 1.

B. Blast Cone and Nozzle Extension

The blast wave was generated by the detonation of an explosive near the apex of a hollow cone. As has been discussed elsewhere (Reference 4), the blast wave thus generated corresponds to that from a spherical blast generated by a larger charge. The ratio of effective charge size to that detonated in the cone is known as the Amplification Factor, and is the ratio of the solid angle of a sphere (4π steradians) to that of the cone. The cone-semivertex angle used in this test was $5^{\circ} 43'$, yielding an ideal amplification factor of 402. That is to say, one gram of explosive gives the same blast strength (i. e., overpressure) at a given distance from the source as would a sphere of 402 grams in free air.

The charge was confined and detonated in a firing block with an outside diameter of 8 inches and an inside diameter of 1 inch.

* Approximately -40°F dewpoint

The blast cone was installed normal to the flow, intersecting a short nozzle extension. This latter extension covered one third of the nozzle circumference and its purpose was to form a smooth junction of the Mach 2 nozzle and the blast cone.

Figure 2 shows a photograph of the cone installed in the receiver tank.

C. Explosive and Initiators

The explosive used in the test program was Pentolite, provided by NWL in the form of pellets (apparently cast) 1/4-inch diameter and in lengths of 1/2 and 2 inches. (50-50) Pentolite is a mixture of equal weights of PETN and TNT and, although obsolete, is frequently used for experimental work. The explosive was initiated by an electric detonator*. A small "booster pellet" of 12 grains of PBX 9407 (about 11 grains of RDX in a plastic binder) was provided by CAL's Weapons Research Department to increase the reliability of the detonator under conditions of poor contact with the explosive. Mechanical coupling of the detonator output was provided by placing a disc, 1/4-inch diameter, 0.002 inches thick, of brass between the booster pellet and the Pentolite.

Detonation transfer between individual pieces of Pentolite was aided by about a half-gram quantity of LX-02 plastic explosive. LX-02 contains 68% PETN in a butyl rubber binder. A schematic representation of the explosive train is shown in Figure 3.

D. Model and Model Support

The model consisted of a cylindrical fuselage with an ogival nose, a 65° delta wing and a 65° delta vertical tail. The wing span was 13 inches.

The model was mounted on a long, relatively springy sting from a very rigid mount attached to the bottom of the receiver tank (Figure 4). The sting could be moved to an angle of 10° to the horizontal and the model could be rolled relative to the sting into three different positions.

An installation photograph is shown in Figure 5.

* Type E-94, Military Specialties Sales, E. I. Dupont de Nemours Co., Inc., Wilmington, Delaware

E. Airflow Rake

The airflow quality in the nozzle was surveyed by means of a pitot survey rake. Nine pitot probes were provided, one on the centerline and four each at three-inch centers either side of centerline in the horizontal plane.

It was possible to alter the axial location of the pitot rake over a distance of about two feet.

A photograph of the installed survey rake is shown in Figure 6.

F. Instrumentation and Data Recording

1. Rake Instrumentation

The pitot survey rake was provided with nine CAL-made piezo-electric pressure transducers. These transducers were used with miniaturized FET* impedance-matching amplifiers, giving sensitivities of order 100 mv/psi. The transducers are acceleration compensated and, when used with suitable low pass filters to remove the high frequency signal due to resonant excitation, offer response of order 1 millisecond. Further descriptions of the transducer and the FET circuit are found in References 5 and 6.

A similar transducer was used to measure the stagnation pressure in the subsonic flow upstream of the throat.

2. Blast-Cone Instrumentation

The blast cone was instrumented with three Kistler type 603A high-frequency-response piezoelectric pressure transducers (Figure 7). The mounting used in these locations was basically the hard type recommended by the manufacturer (Figure 8(b)). Kistler charge amplifiers were used with these transducers.

During the static cone calibrations, reflected overpressure was measured by a pcb type 112 MO1⁺ pressure transducer mounted in a rigid circular plate which was suspended from the ceiling of the receiver tank by

*Field Effect Transistor

⁺pcb Piezotronics, Inc., P.O. Box 33, Buffalo, New York 14225

means of cables. This transducer is internally very similar to the Kistler Type 603A, its main difference being a smaller overall length and the provision of pigtail leads rather than a connector. The mounting technique was similar to that used for the Kistler except that the washer upon which the transducer was seated was made of Boron Nitride^{*} and that the compression of the transducer was achieved by a plate with small screws rather than a single hollow pusher screw (Figure 8(a)). This mounting technique, together with the previously-mentioned smaller transducer length allows installation of a transducer in a more confined space than is possible with a Kistler transducer. This mounting technique was also used for the transducers in the model (see section F-3 below) and is discussed in Appendix B.

3. Model Instrumentation

The delta-wing model was provided with four Kistler Type 603A transducers and four of the pcb type 112 MO1, both mounted as discussed above (section F-2). In order to minimize electrical noise generated by cable motion, each was provided with a compact, solid-state source follower^{**} pcb Model No. 402A, which was mounted as close as possible to the transducer. A photograph of a typical transducer installation, showing the source follower, is seen in Figure 9. The transducer locations are shown in Figure 10.

4. Data Recording

All pitot-survey, blast-cone, and model data were recorded on Tektronix Type 502 and 535 oscilloscopes with Polaroid Land cameras. Electrical filters were used on most channels; these are discussed in Appendix A.

G. Flow Visualization

Because the blast cone is mounted horizontally, it was necessary to develop a vertical schlieren/shadowgraph flow visualization system. The system, shown schematically in Figure 11, is a double-pass conical layout.

^{*} Selected for its properties of high rigidity and good electrical insulation.

^{**} A source follower (sometimes called a line driver or impedance converter) is similar to a cathode follower in purpose, i. e., it lowers the output impedance to about 100 Ohms.

The spherical mirror is placed on the floor under the receiver and the flat turning mirror, light source, knife edge and camera are hung from the ceiling structure of the Laboratory. Thus none of the components are attached to the external flow system itself. A modified Graflex shutter was used, which opens for about 4 milliseconds, the spark being actuated independently. In view of the need for rapid availability of the photographs Polaroid Type 57 sheet film was used.

III. TEST PROCEDURE

A. Calibration of Pressure Transducers

1. Bench Calibrations

The CAL-made pressure transducers were calibrated on the bench, using a quick-acting valve which released air from a pressurized bottle to the transducers in the pitot probe heads. The pressure in the storage bottle was read on a precision dial gage. The Kistler and pcb transducers were calibrated with a deadweight tester, using the actual input lead lengths and amplifier system which would be later utilized in the model or blast cone.

The voltage variation (i. e., voltage output versus applied pressure) of the transducers is linear over the range of pressures encountered in the tests. These calibrations, in conjunction with the estimated values of expected pressures, also provide the basis for adjusting the settings of oscilloscopes to achieve optimum readability.

The detailed calibration data are kept on file at CAL.

2. Shock Tube Tests

An evaluation of the dynamic response of the Kistler and pcb transducers was performed using a small cold-air-driven shock tube*. This provides an essentially pure step pressure input to the transducer and allows a selection of suitable filters for the test program. A detailed description of these tests is found in Appendix A.

B. Test Program

A total of 15 static cone calibrations, 5 airflow calibrations, and 24 data-producing runs were made. Tables 1 and 3 present summaries of the run schedules of the cone calibration and model data phases of the program.

* other types of transducers were also evaluated and rejected.

C. Test Operation

1. Blast Cone

The charge, consisting of one or more Pentolite pellets, was supported in a rigid foam rod. Both the internal and external diameters of this rod were such as to ensure a tight fit with the Pentolite and firing block respectively, in order to minimize the motion of the charge.

A Mylar diaphragm, 0.002 inches thick was installed between the firing block and the blast cone for the latter part of the test program. This diaphragm, replaced prior to every run, separated the charge from the receiver tank and was used for two reasons. Firstly, the flow of air into the cone during the starting processes of the nozzle was prevented from disturbing the charge, possibly introducing an excessive gap between the charge and the initiator. Secondly, the pressure ambient to the charge remained atmospheric, whereas the receiver tank was initially at very low pressure in order to facilitate starting. Initiation of the charge under conditions of poor contact with the initiator is much more reliable when the ambient pressure is higher.

2. External Flow System

Before a run, the supply tube and the receiver tank are separated by Mylar diaphragms and the receiver tank evacuated to less than 10 mmHg in order to facilitate nozzle starting. After the supply tube has been filled to the desired pressure the run is initiated. The fireswitch opens a solenoid valve which allows Helium at 200 psia to actuate a cutter. The cutter, in the form of a cruciform-shaped knife, cuts the diaphragm about 60 milliseconds after the fireswitch is operated and the triangular diaphragm "petals" thus formed are rapidly pushed to the side of the tube, any broken pieces being restrained by a wire mesh immediately downstream. Flow is established in the test section 10 to 20 milliseconds after diaphragm rupture, leaving at least 20 milliseconds of steady flow.

The fireswitch also actuates an electronic delay which then initiates the detonator and also starts the opening of the camera shutter. This time delay is adjusted so that the blast wave arrives in the test section

very shortly before the end of steady test time, in order to ensure that the model flow has as long a time as possible to equilibrate. After the charge has detonated, the blast passes the first pressure transducer in the blast cone, PS1, and the output from this triggers some of the oscilloscopes. Others, particularly the fast-sweep oscilloscopes recording the model pressure data, are triggered after a suitable delay from the cone exit pressure (PS3). This transducer also initiates the spark source for flow visualization.

IV. DATA REDUCTION

Both CAL-made, and Kistler and pcb pressure transducers measure the difference between initial ambient pressure and the local pressure suddenly applied in the test. Therefore, to obtain the true rake pitot pressure, the initial receiver pressure is added to the measured pressure. Similarly, the blast pressures recorded on the model are changes in pressure over the ambient, flow-generated, model pressure.

The cone calibration data obtained is also recorded as pressure change from ambient, however, this is consistent with the usual convention of blast wave testing.

The magnitude of the peak overpressure was corrected to account for the limited frequency response of the transducer system. This correction is discussed in Appendix A.

V. PRESENTATION OF DATA

A. Cone Calibration

The schedule of cone calibration runs is shown in Table 1.

Typical cone-wall-static and reflected-shock pressure-time histories are presented in Figure 12. The appearance of these data confirm that the blast wave is well-formed and has the characteristics of a spherical blast at both sea level and 30,000 ft. simulated altitude (240 mmHg). However, at 70,000 ft. simulated altitude (33 mmHg) the pressure-time histories did not demonstrate these characteristics, as seen in Figure 12(c). The reason for this is unknown, but may be related to the greater difficulty in obtaining good detonation transfer at low ambient pressure. The diaphragm separating the firing block and the blast cone, mentioned in Section III-C(1), was not utilized at the time of the calibrations: a modification to the firing block was necessary to do this, and this expense was not warranted at that time.

The performance of the blast cone is presented graphically in Figures 13(a) and 13(b). The theoretical line is based on the charge-weight and altitude correlation of Reference 7. Lines of 70% efficiencies are also presented. It is seen that the cone static pressures (Figure 13a) are consistent with an efficiency of between about 70% and 100%, i. e., the cone behaves as if between 70% and 100% of the charge is detonated. Any deficiency is probably due to shock attenuation caused by viscous effects as well as the fact that the charge is not a true spherical sector. This efficiency may be compared with previous experience with cones of other vertex angles (Reference 8) in Table 2.

The reflected shock pressure as a function of charge weight is shown in Figure 13b. These data are taken at the nozzle centerline, i. e., 20 7/8" from the cone exit, where some drop in performance would be anticipated because of the free expansion beyond the exit but none is detectable. Times of shock arrival (at sea level only) are presented in Figure 14. The present data agree well with the correlations of Reference 9 which presents results

from spherical charges in free air. A shadowgraph photograph, showing the blast wave approaching the flat plate, is shown in Figure 15.

B. Nozzle Airflow

Pitot surveys of the nozzle airflow were made at two simulated altitudes and two axial locations. A representative plot of pitot/total pressure ratio as a function of radial location is presented in Figure 16. The mean of this ratio is also shown, together with the lines representing variations of $\pm 5\%$. The mean level was used to calculate the average flow Mach number, using the tables of Reference 10. A small drop of total pressure due to the wake from the centerbody is seen near the centerline, but this only represents a 2% change in flow Mach number. The axial Mach number gradient is about 5% in two feet; theory predicts about 8%. A schlieren photograph of the flow over the rake is shown in Figure 17.

C. Model Data

The schedule of model runs is shown in Table 3. Typical model overpressure time histories are shown in Figure 18. In all cases, the baseline is the ambient, flow-generated, pressure on the model at that location. In the case shown, which is a run at a simulated altitude of 35,000 ft., the pressure after the arrival of the blast wave rises rapidly and then falls below ambient. This is typical of spherical blasts at such altitudes. The wing pressure data (locations 7 and 8) for this run are especially interesting where the reflection of the blast from the vertical tail is clearly seen.

The variations of peak overpressure at various locations as a function of model attitude are presented graphically in Figures 19 (a) through 19 (h). The charge weight and simulated altitude remained fixed in this group of runs. Figure 19 (a) shows this variation for position P1 on the nose. The data at this location were unusual in that the time history did not typically exhibit the expected blast wave shape. There was usually no sharply-defined peak, but rather a pressure plateau of 0.5 to 1.5 milliseconds duration (Figure 18 (a)). The plotted data are interesting in that they show that the peak pressure rises as the model is rolled; the peak being about four times greater when the transducer sees the blast edge-on than when it is exposed to the blast face-on. The data from the two fuselage locations (P2 and P5)

are presented in Figures 19(b) and 19(e). These show the more expected behavior; the face-on pressure being larger than the side-on. A theoretical line from Reference 11 is also presented; however, some rather sweeping assumptions are implied by this line. The first assumption is that the pressure at a point on a cylinder is the same as on an infinite plane tangent to the cylinder at that point. This assumption is similar to the tangent-wedge assumption used in hypersonic flows (see, for example, a discussion of this in Reference 12). The second assumption is that the blast cone extends all the way to the model and the third is that the flow field over the model does not interact with the blast wave (i. e., that the flow and blast may be superimposed). Curves for a cone of 100% efficiency and 70% efficiency are shown. The agreement at location P2 is not good, but the trend is predicted fairly well. The data at location P5, however, agree surprisingly well with this crude theory and the trend is well predicted. The assumptions are of course better suited to prediction of the "upblast"* wing location (P7) and these data are discussed below.

Locations P3 and P4 were in the wing root, the former being on the fuselage, the latter on the wing. The data are compared with the theory of Reference 13 in Figures 19(c) and (d). Again the assumptions of an infinite ground (represented by the wing) and of superimposition were made. In view of the fact that the theory applies to a square corner and that the corner in the experiment contained a fillet formed by the fuselage, the agreement is rather good and the trends again are well predicted. The same theory is compared with the data near the root of the fin (position P6) in Figure 19(f). Here the assumption of a vertical wall is far from reasonable and the data accordingly lies far from theory, especially at the -45° roll position. One would expect that the -45° position would be the most difficult to predict: the extremely large pressure ratios calculated in Reference 13 are caused by the collision of two strong shock waves which occurs exactly in the corner, the pressure ratios being much lower anywhere else. Clearly in the more

* Here "upblast" refers to the wing position not sheltered from the blast by the fin. The other position (P8) will be referred to as the "lee" side.

complex geometry used in the reported tests, the simple shock collision model used in the reference does not apply and a smaller pressure multiplication would be expected.

The "upblast" wing location data (P7) are plotted in Figure 19 (g) and the theory of Reference 11 previously mentioned is also presented. The agreement is good. The data from the "lee" side location (P8) are also compared with this theory in Figure 19 (h) and, as would be anticipated, the shielding effect of the fin causes the overpressures to be lower than on P7. Peak overpressures, as a function of model roll angle, at other altitudes, are also presented in Figure 19, together with the theoretical results for these conditions.

The variations of peak overpressures with altitude are seen in Figure 20. The model was fixed at the -90° roll, zero angle-of-attack position, and the charge weight fixed at 5.7 grams for this series of runs. The theoretical incident and reflected overpressure variations from Reference 7 are included for comparison. Of all positions, numbers P5, P7, and P8 should agree best with the theoretically reflected overpressure. The agreement is not good for any of these; the trend of the wing data being completely at variance with the prediction. The experimental trend is, however, quite clear and one must conclude that there is an effect due to the airflow over the model, an effect which is particularly strong on the wing. One must also conclude that the relatively good agreement of absolute levels in Figure 19, referred to above, is fortuitous.

The effect of various charge weights at fixed altitude and model aspect was also investigated. The data from these runs are plotted in Figure 21 and, again, the theoretical incident and reflected overpressure lines are included where useful. The trend here is clearly obeyed well, the absolute agreement in the wing data being quite good. The fact that this is so adds further credence to the above conclusion that a flow interaction does occur.

In Figures 19, 20, and 21, data are also included from the runs made at 9° effective angle of attack for the model. These data are identified by flagged symbols. There did not appear to be a very strong effect due to angle of attack, no trend being discernable. It is probable, however, that larger angles of attack would have more effect.

An additional limitation to all the model data remains to be mentioned: the repeatability, or lack thereof, of the blast strength. It had been intended that the data in Figures 19, 20, and 21 would be presented in the form of pressures nondimensionalized to the incident overpressure measured at the cone exit. However, these measured pressures, at a given simulated altitude and charge weight, exhibited a standard deviation of 17% at PS3 and 18.5% at PS2, considerably more than would be expected due to charge nonuniformities alone. Further, the reading at PS2 averaged 120% higher than at PS3, the latter being much closer to theory. It is thought that the difficulties experienced were due to locally-strong interactions of the blast wave with the complex flow field at the cone exit. Oscilloscope records of the pressures at these locations due to the supersonic flow prior to the arrival of the blast wave show considerable unsteadiness. Electrical difficulties also prevented the recording of incident overpressure at PS3 on one third of the runs. The small remaining amounts of data, when nondimensionalized by this overpressure do not display any reduction in scatter, or any improved agreement with theory. The nondimensionalized data are, accordingly, not presented here.

A shadowgraph photograph of the blast wave approaching the model is shown in Figure 22. The bow shock and wing root shock due to the airflow are also clearly visible.

D. Limitations of the Experimental Technique

There are two major limitations to the experimental technique employed in the reported tests. The first is present in most ground-testing techniques which attempt to simulate a blast normal to the flow velocity (or target flight direction). This is that the blast source is stationary relative to the target. Now this is not a poor representation of some interception techniques (e. g., a lead-pursuit interception by a missile little faster than its target); however, the result is that the blast wave is not normal to the target*.

*The effect of the flow on the blast wave is clearly seen by comparing Figures 15 and 22.

The second limitation of this particular technique is that the blast wave must traverse regions of variable, and unsteady, local properties. Unsteadiness will be greatest near the cone exit, where an extremely complex flow field exists, and the interactions will be most severe in that region. The existence of a large discrepancy between incident overpressures measured at the two positions at the cone exit (see section V-C) is evidence of this. On the other hand, examination of the shadowgraph pictures do not show any large distortion of the blast wave, other than that expected from the flow as mentioned above.

Other than these limitations, the technique appears to offer considerable advantages, especially simplicity and low cost.

VI. PRECISION OF DATA

A. Precision of Pressure Data

The calibration inaccuracies and transducer nonlinearities give rise to errors of about $\pm 2\%$ and the recording and reading errors about $\pm 1\%$ each. The expected "Most Probable Error" based on these figures is therefore estimated at about $\pm 2\frac{1}{2}\%$. The repeatability achieved in typical shock tunnel and rocket tests with CAL-made and Kistler transducers appears to be about $\pm 5\%$. It is not known why this is larger than the estimate.

CAL has no previous experience with pcb-type transducers, but based on the fact that their design and construction are almost identical to the Kistler, it is expected that their repeatability would be similar.

B. Precision of Correction for Limited Frequency Response

The correction for the limited frequency of the transducer system, discussed in Appendix A, also provides an error. In some cases the correction is as large as 30%, but is usually of order 10 to 20%. The accuracy of this correction is estimated at $\pm 20\%$, yielding typical errors of $\pm 4\%$ due to corrections.

VII. CONCLUSIONS AND RECOMMENDATIONS

The feasibility of investigating the effects of blasts from chemical explosives on vehicles in a supersonic flow by means of a short-duration wind tunnel coupled to a conical blast generator has been demonstrated, and experimental data on the effects of model attitude, altitude and charge weight obtained. After examination of these data, the following conclusions may be made:

1. The blast-generating cone behaves according to previously-established scaling laws.
2. The effect of roll angle on peak overpressure on the model is in accordance with the trend predicted by simple theories for stationary targets.
3. Increasing charge weight increases overpressure in the manner expected from theory.
4. There appears to be only a slight effect due to the interaction of the blast wave with the flow field about the model, discernable because the effect of altitude is generally to decrease the reflected overpressures on the model, whereas theory for stationary targets predicts a slight increase.
5. The test technique is simple and efficient: when the blast generator alone was operated, four runs per day were obtained with a crew of one or two people.

On the basis of the problems experienced and the search made in the literature for theoretical solutions appropriate to the program, the following recommendations are made:

1. One limitation of the technique was the interaction of the blast wave with the complex flow field at the blast cone exit, making it difficult to measure the incident overpressure. As it is desirable to measure this on every run in order to verify that the blast generated is repeatable, or to correct the data if it

is not, an improvement is needed. It is recommended that in any future tests, a cone static pressure transducer be installed some distance into the cone. This offers the double advantage that the overpressure measured is higher and that the flow disturbances are less. Although such a transducer would not aid in the determination of incident overpressure at the model, it would allow a check to be made on run-to-run repeatability.

2. The problem of the effect of the flow on the blast wave, distorting it so that it does not impinge on the model normal to its axis, warrants further investigation. Reference 14 presents numerical solutions for a situation closely resembling the reported tests and the computer program presented therein could be applied in order to find a model position where the blast is normally incident and in order to provide an estimate of the loss of blast strength. Further investigation should include tests to determine whether model position does strongly effect the resultant model overpressures.
3. In view of the extremely limited amount of theoretical or experimental data on the overpressures on simple shapes, such as cylinders and surfaces shielded by other bodies or surfaces, the technique should be used to obtain such experimental data. The method offers the advantage of a well-controlled environment and makes possible the investigation of altitude effects.

REFERENCES

1. Ludwig, H., "The Tube Wind Tunnel - A Special Type of Blowdown Tunnel," AGARD Report 143, July 1957.
2. Cable, A. J. and Cox, R. N., "The Ludwig Pressure-Tube Supersonic Wind Tunnel," The Aeronautical Quarterly, Vol. 15, 1963, pp. 143-157.
3. Sheeran, W. J., Hendershot, K. C., and Wilson, H. B. Jr., "Applications of a Tube Wind Tunnel in Supersonic Testing," Proc. AIAA 4th Aerodynamic Testing Conference, Cincinnati, Ohio, April 28-30, 1969, AIAA Paper No. 69-335.
4. Filler, W. S., Physics of Fluids 3, 444 (1960).
5. MacArthur, R. C. and Martin, J. F., "Use of Field Effect Transistors in Shock Tunnel Instrumentation Circuits," Proc. IEEE 2nd International Congress on Instrumentation in Aerospace Simulation Facilities, Stanford University, California, August 1966.
6. Bogdan, L., "Instrumentation Techniques for Short-Duration Test Facilities," CAL Report WTH-030, March 1967.
7. Dewey, J., and Sperrazza, J., "The Effect of Atmospheric Pressure and Temperature on Air Shock," Aberdeen Proving Ground, B. R. L. Report No. 721, May 1950
(see also:
Morton, H. S. and deHaas, N., "Nomographic Presentation of Blast Data on Spherical Charges of 50/50 Pentolite from Sea Level to 50,000 ft., The Johns Hopkins Univ., Applied Physics Lab. CM-726, April 1962).
8. Culbertson, D. W., "A Description and Predicted Performance of a Conical Shock Tube Nuclear-Blast Simulator," Proceedings of the Conference on Military Applications of Blast Simulators, Defense Research Establishment, Suffield, Alberta, July 1967.
9. Goodman, H. J., "Compiled Free-Air Blast Data on Bare Spherical Pentolite," Aberdeen Proving Ground B. R. L. Report 1092, Feb. 1960.
10. Ames Research Staff, "Equations, Tables, and Charts for Compressible Flow," NACA Report 1135 (out of print).
11. Glasstone, S. (Ed.), THE EFFECTS OF NUCLEAR WEAPONS (Revised Edition), U. S. A. E. C., April 1962.

12. Chernyi, G. G., INTRODUCTION TO HYPERSONIC FLOW,
Academic Press, 1961, p. 113.
13. Dresner, L., "Peak Overpressure at the Foot of a Vertical Wall
Facing an Air Blast," Journal of Applied Physics, Vol. 40,
No. 4, 15 March 1969, pp. 1945-1949.
14. Tyler, L. D. and Zumwalt, G. W., "Numerical Solutions of the
Flow Field Produced by a Plane Shock Wave Emerging into a
Crossflow," Sandia Corporation, Report SC-DC-65-1916,
August 1965.

Table 1
RUN SCHEDULE
(STATIC CONE CALIBRATIONS)

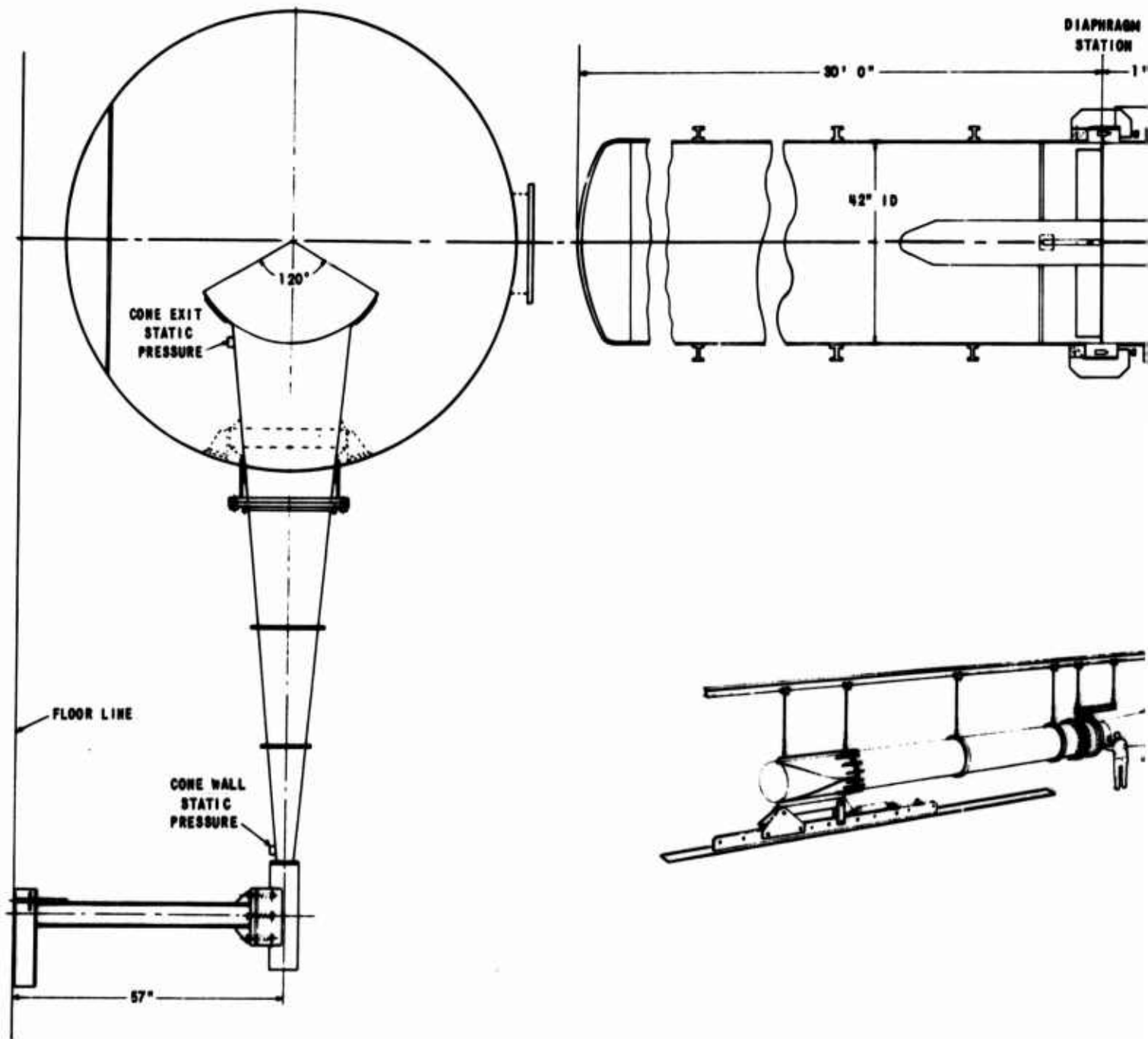
RUN NO.	SIMULATED ALTITUDE (kft)	CHARGE WEIGHT (gms)	COMMENTS
4	0	2.7	NO DATA
5	↓	2.9	
6	↓	2.9	
7	↓	5.7	
8	↓	11.3	NO DATA ON PRI
9	30	2.9	
10	70	2.9	
11	70	2.9	
12	30	5.7	NO DATA ON PRI
13	30	5.7	
14	0	16.9	
15	30	11.3	
16	70	5.7	NO DATA ON PRI
17	70	11.3	
18	30	11.3	
19	30	16.9	

Table 2
PERFORMANCE OF CONICAL SHOCK TUBES
(REFERENCE 8)

CONE SEMI- VERTEX ANGLE (deg)	AMPLIFICATION		EFFICIENCY (%)
	IDEAL	ACTUAL	
22	110	60	55
2	10,000	3,000	30
0.637	1.296×10^5	3×10^4	23

Table 3
RUN SCHEDULE
(MODEL-DATA RUNS)

RUN NO.	SIMULATED ALTITUDE (kft)	CHARGE WEIGHT (gms)	MODEL ANGLE OF INCIDENCE (α°)	MODEL ROLL ANGLE (ϕ°)	COMMENTS
27	35	5.7	0	-90	NO FLOW, TRANSDUCERS COVERED
28	↓	↓	↓	↓	NO DATA, TRANSDUCERS UNCOVERED
29	↓	↓	↓	↓	REPEAT OF 28, NO DATA
30	↓	↓	↓	↓	REPEAT OF 29
31	↓	↓	↓	↓	WITH FLOW, NO DATA
32	↓	↓	↓	↓	REPEAT OF 31, NO DATA
33	↓	↓	↓	↓	REPEAT OF 32, NO DATA
34	↓	↓	↓	↓	NO FLOW, REPEAT OF 30
35	↓	↓	↓	↓	WITH FLOW, NO DATA
36	↓	↓	↓	↓	NO DATA
37	↓	↓	↓	↓	GOOD DATA
38	↓	↓	↓	-45	GOOD DATA
39	↓	↓	↓	↓	REPEAT OF 36
40	50	↓	↓	↓	
41	50	↓	↓	↓	REPEAT OF 40
42	35	↓	↓	0	
43	↓	↓	9	0	
44	↓	↓	↓	-45	
45	↓	↓	↓	-90	NO DATA
46	↓	↓	↓	↓	REPEAT OF 45
47	↓	↓	0	↓	REPEAT OF 37
48	↓	↓	↓	↓	REPEAT OF 47
49	↓	↓	↓	↓	REPEAT OF 47
50	↓	↓	↓	-45	
51	↓	↓	↓	0	REPEAT OF 42
52	43	↓	↓	-90	
53	↓	↓	↓	↓	REPEAT OF 52
54	↓	↓	↓	↓	REPEAT OF 52
55	63	↓	↓	↓	
56	35	2.9	↓	↓	
57	↓	11.3	↓	↓	
58	↓	15.9	↓	↓	
59	63	5.7	↓	↓	REPEAT OF 55



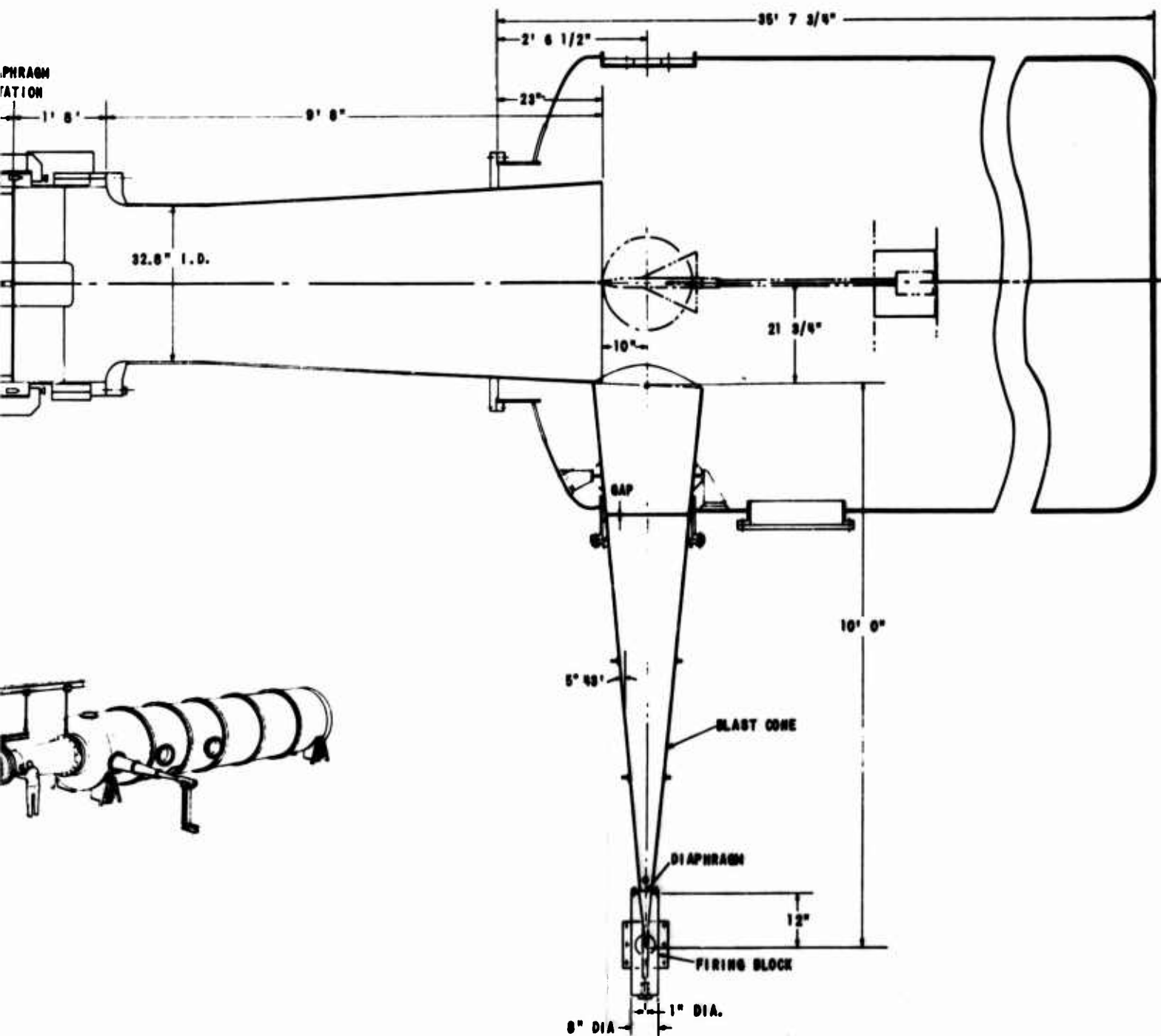
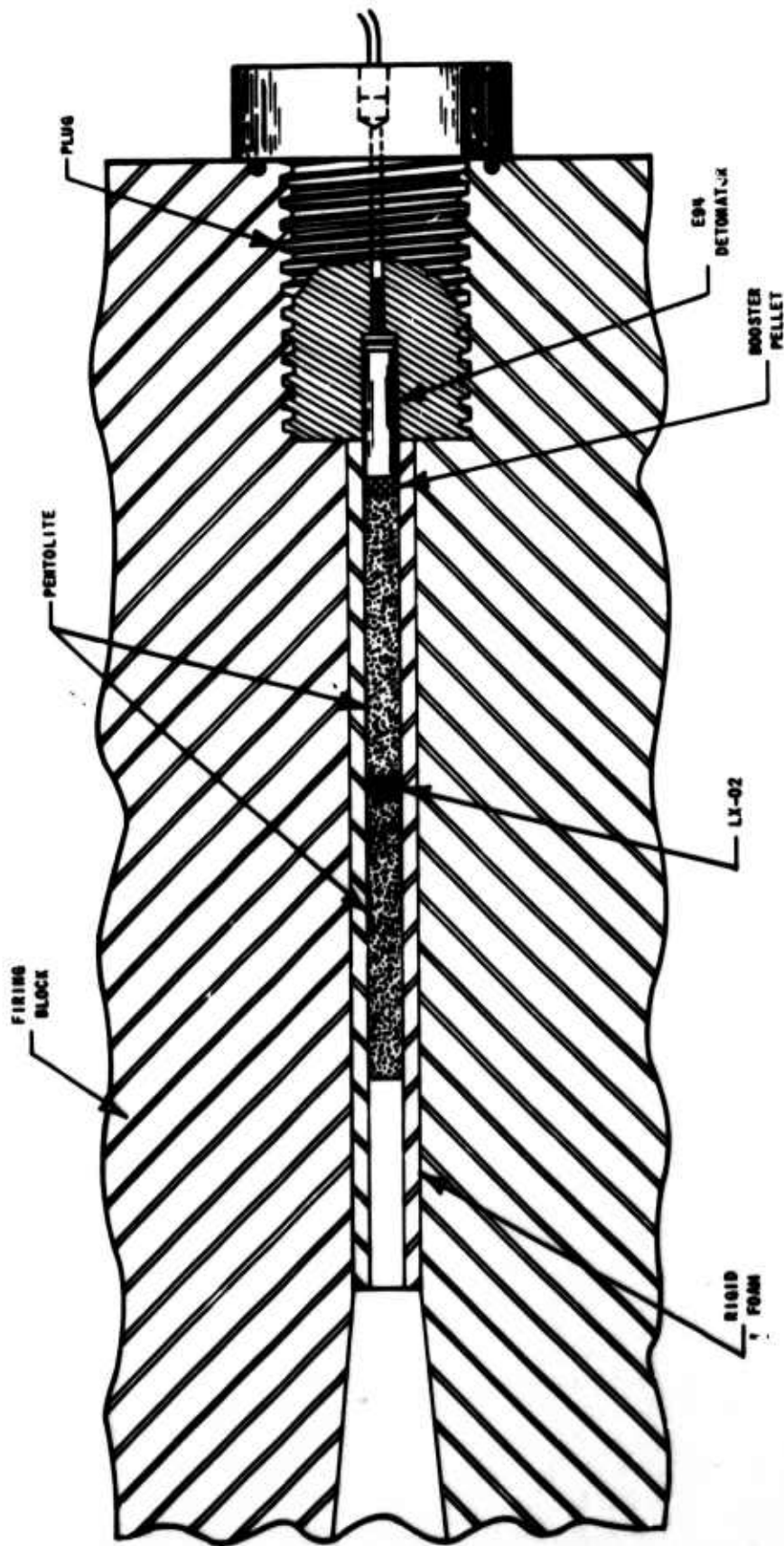


Figure 1 GENERAL ARRANGEMENT OF THE EXTERNAL FLOW SYSTEM AS MODIFIED FOR BLAST WAVE TESTS.



49353

Figure 2 BLAST CONE PHOTOGRAPH



NOT TO SCALE

Figure 3 SCHEMATIC OF EXPLOSIVE TRAIN



Figure 4 MODEL INSTALLATION

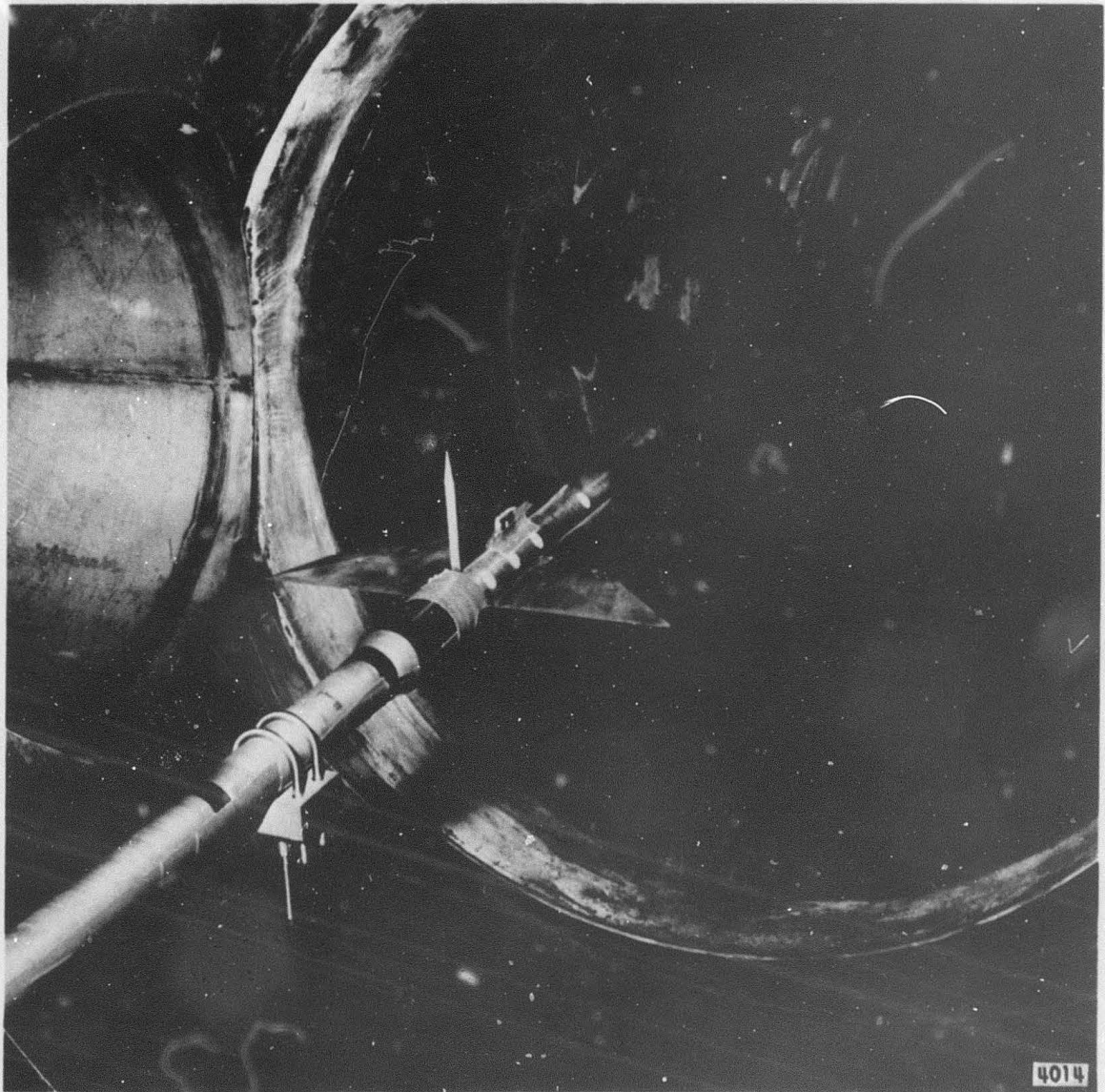
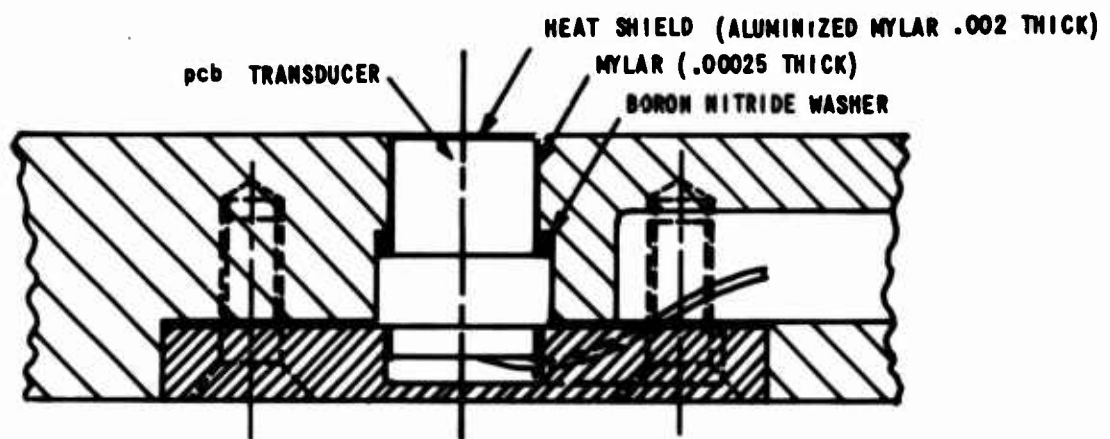


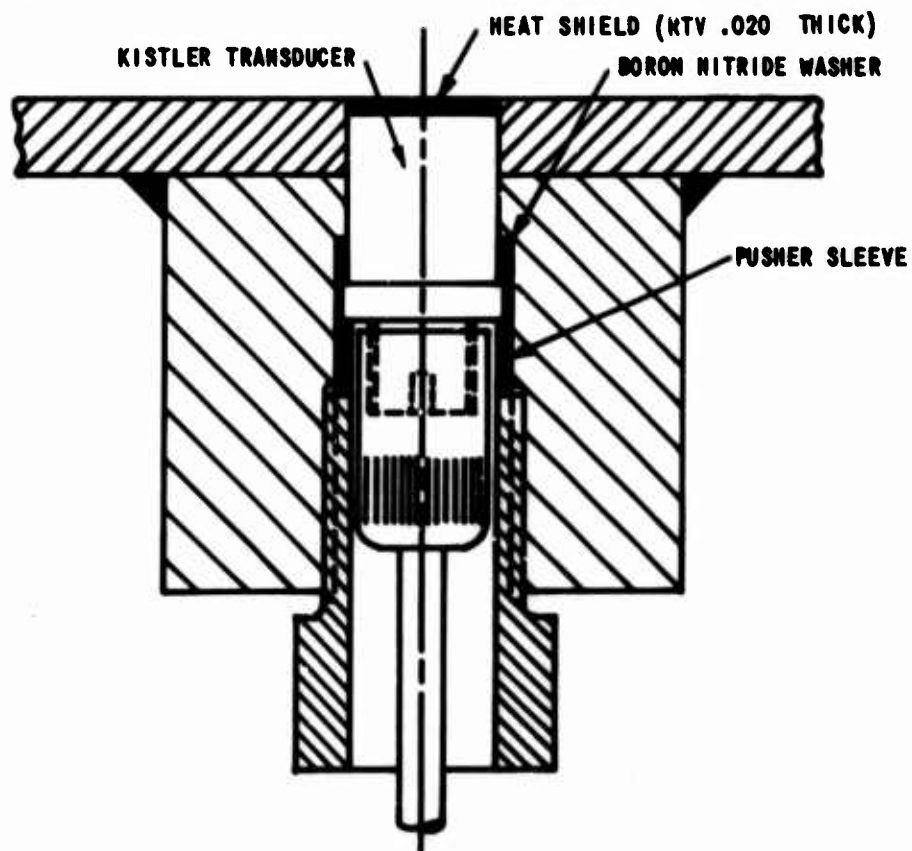
Figure 5 MODEL INSTALLATION PHOTOGRAPH



Figure 6 PITOT SURVEY RAKE INSTALLATION PHOTOGRAPH

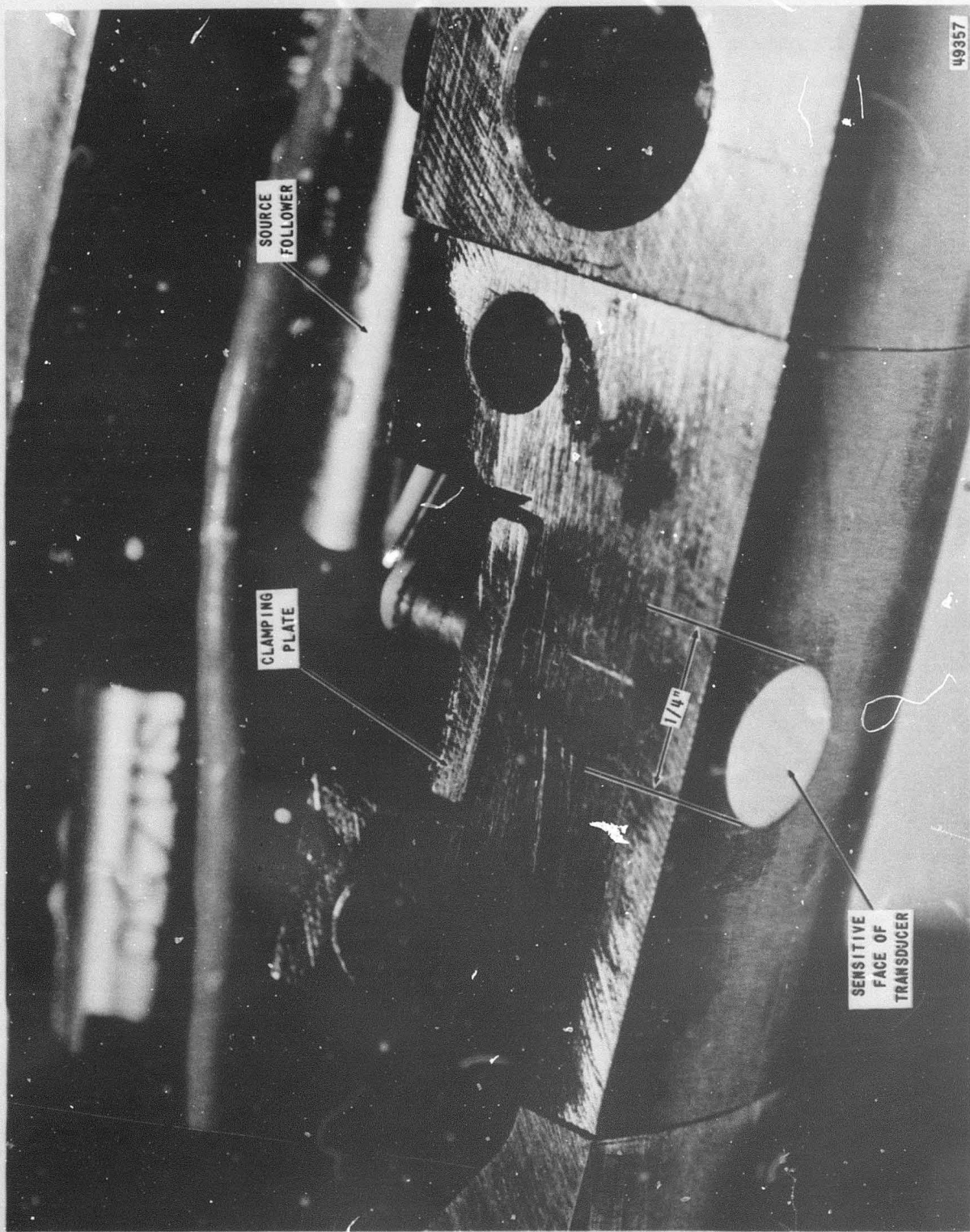


(a) TYPICAL MOUNTING TECHNIQUE USED IN MODEL



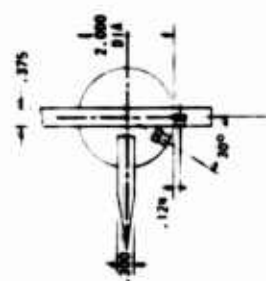
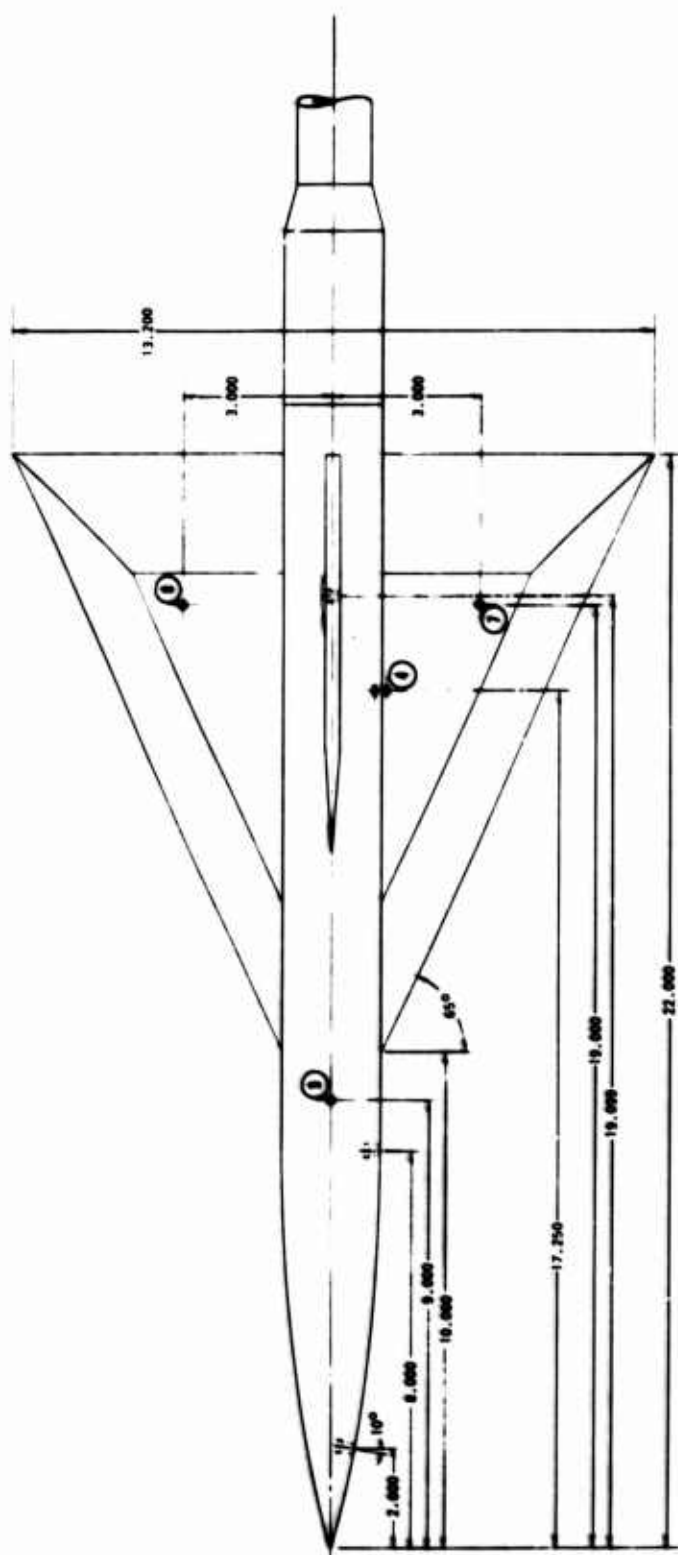
(b) MOUNTING TECHNIQUE USED IN BLAST CONE

Figure 8 TRANSDUCER MOUNTING TECHNIQUES



49357

Figure 9 TYPICAL TRANSDUCER INSTALLATION SHOWING MINIATURE SOURCE FOLLOWER CIRCUIT



ALL DIMENSIONS IN INCHES
 1/2" TYPICAL

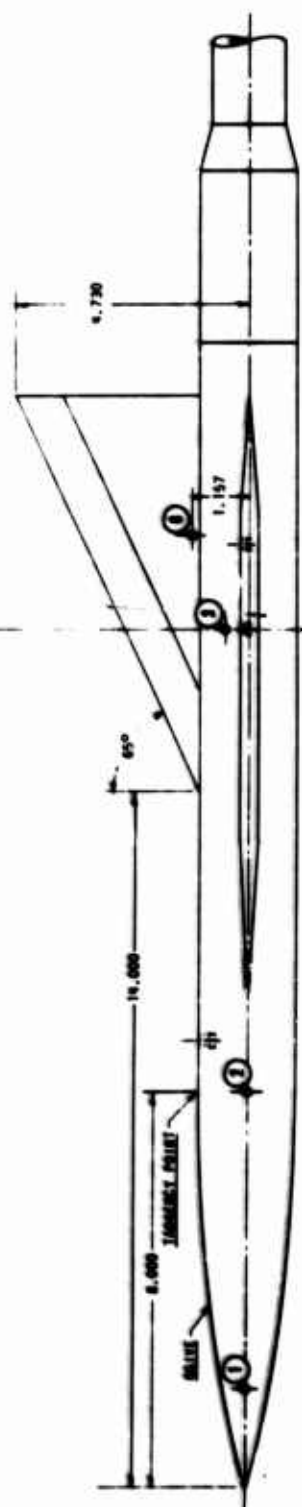


Figure 10 MODEL INSTRUMENTATION LOCATIONS

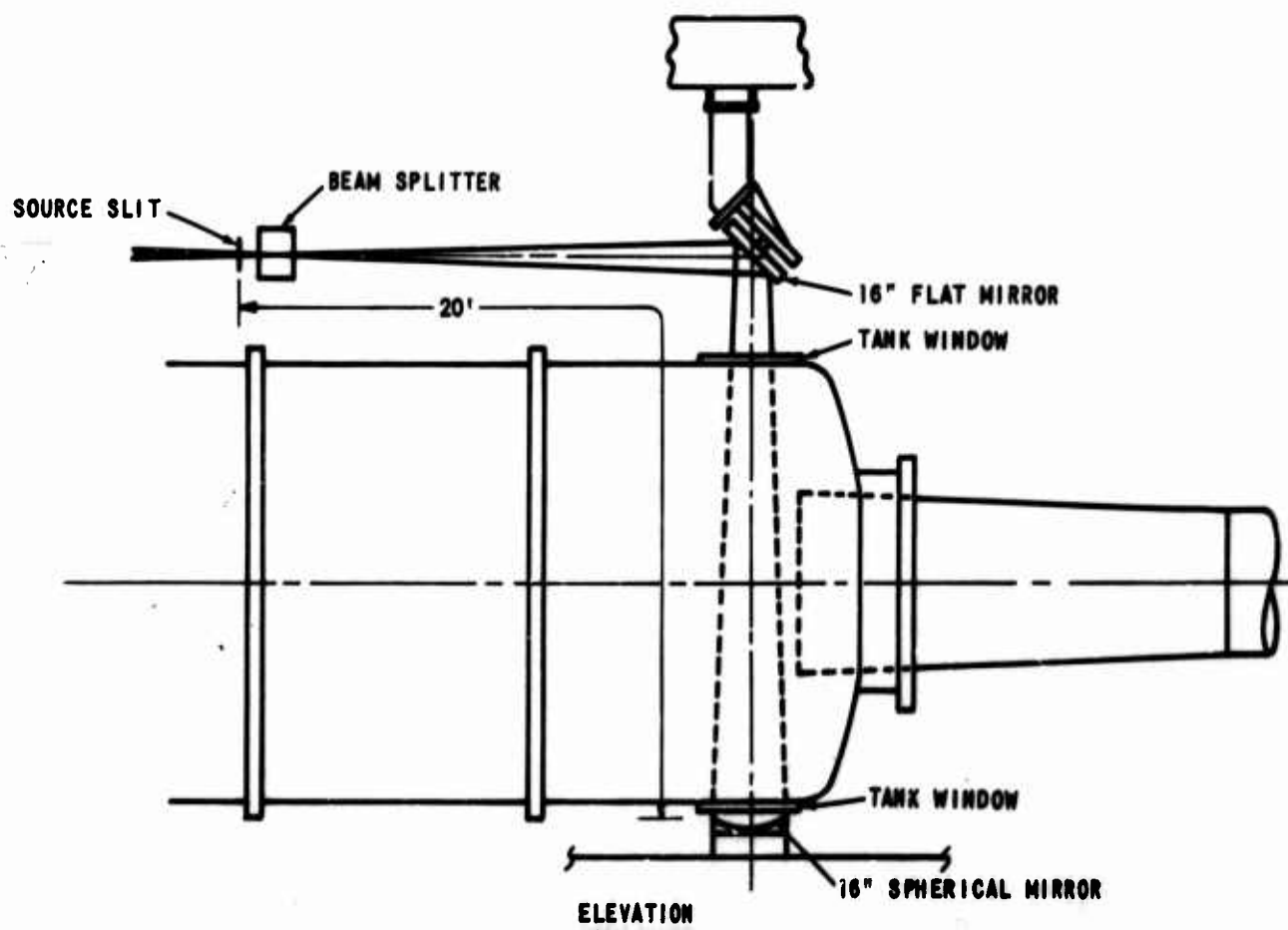
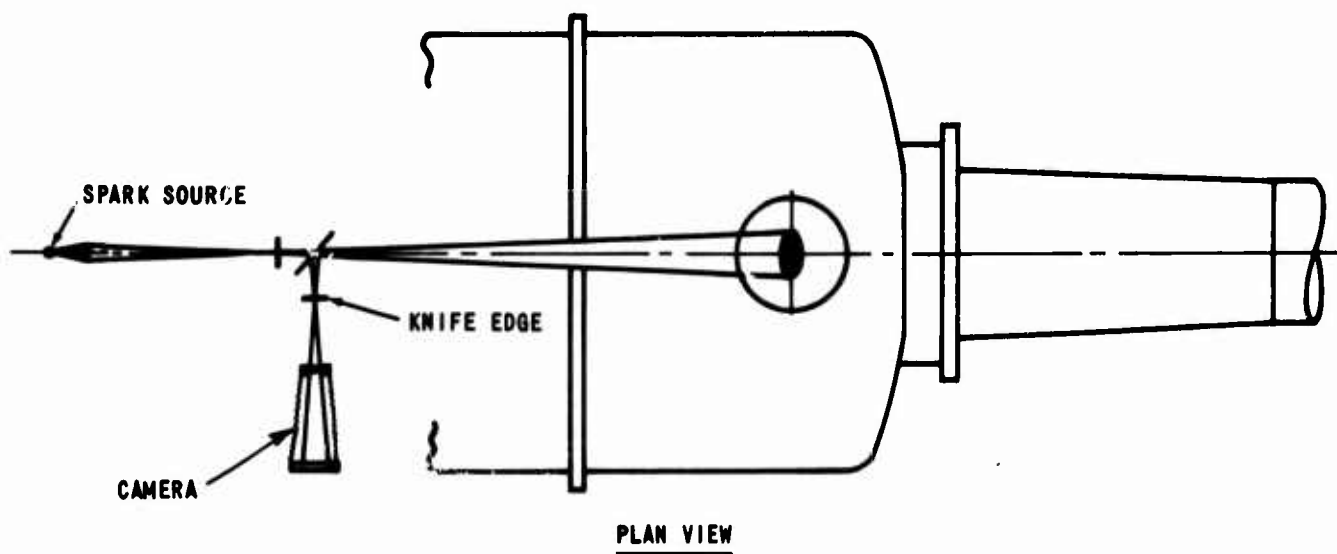


Figure 11 SCHEMATIC OF FLOW VISUALIZATION SYSTEM

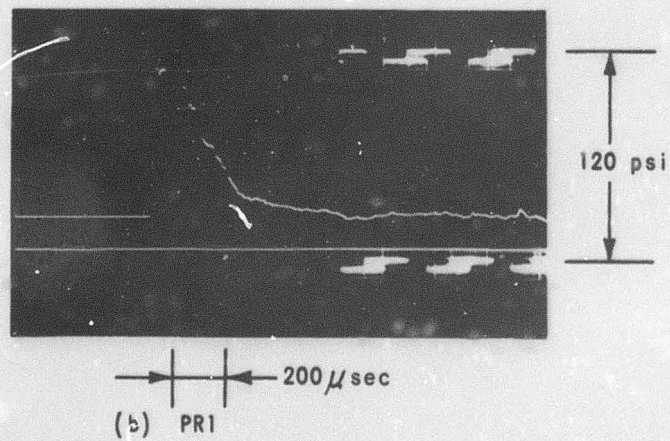
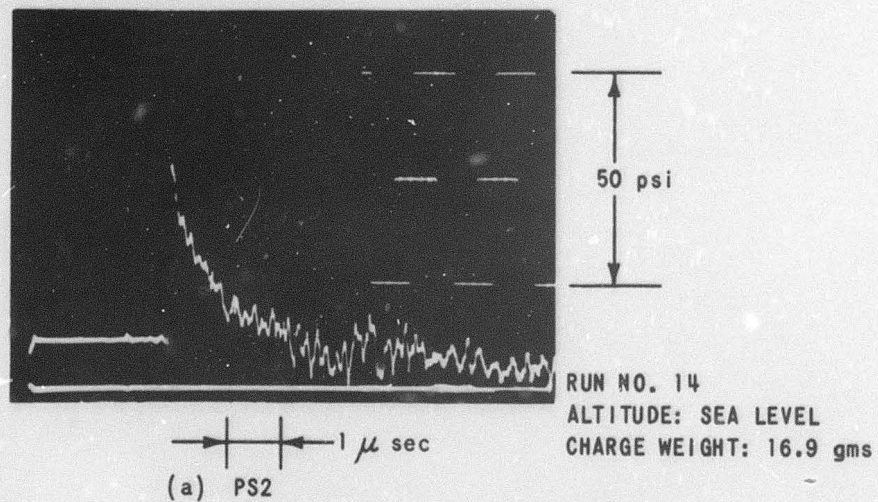
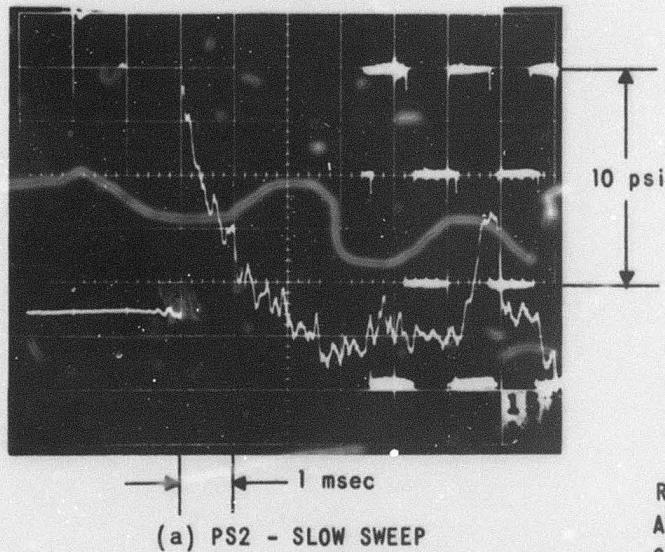


Figure 12a OSCILLOSCOPE RECORDS FROM A STATIC,
CONE CALIBRATION RUN (SEA LEVEL)



RUN NO. 9
 ALTITUDE: 30 Kft
 CHARGE WT: 2.9 gms.

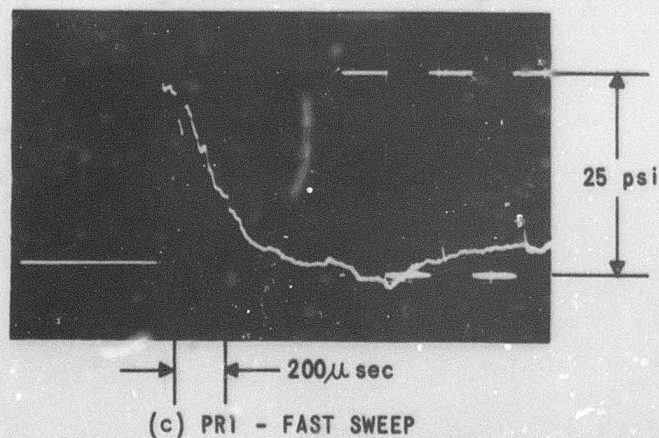
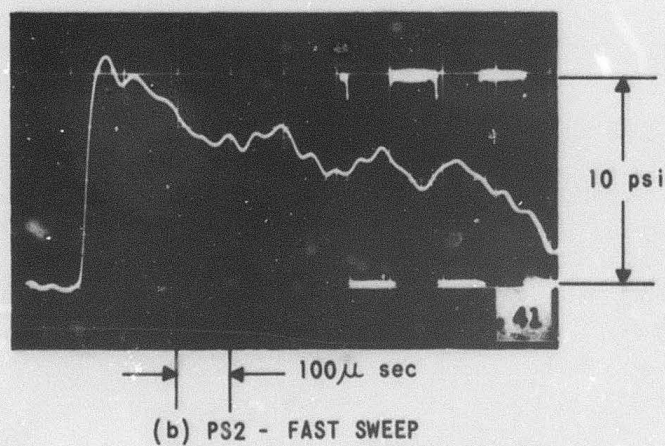


Figure 12 b OSCILLOSCOPE RECORDS FROM A STATIC,
 CONE CALIBRATION RUN (30 Kft)

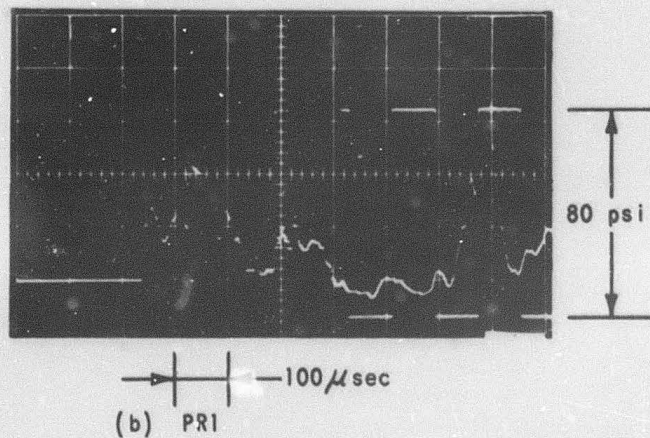
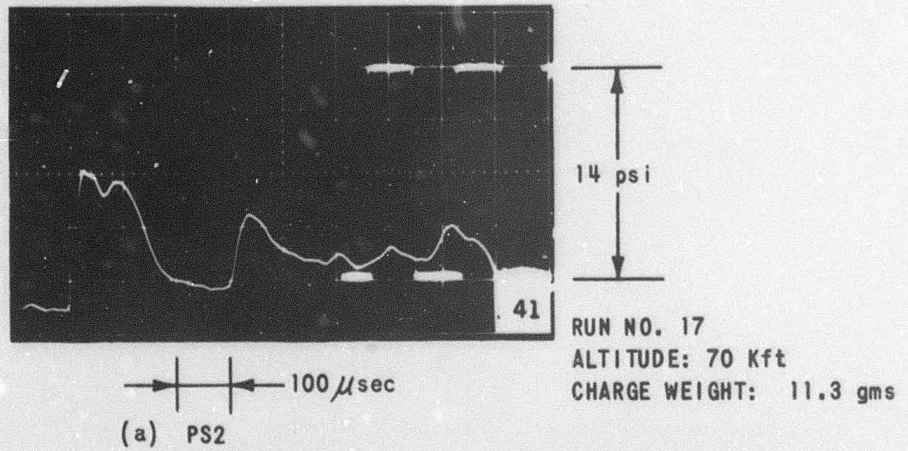


Figure 12c OSCILLOSCOPE RECORDS FROM A STATIC,
CONE CALIBRATION RUN (70 Kft)

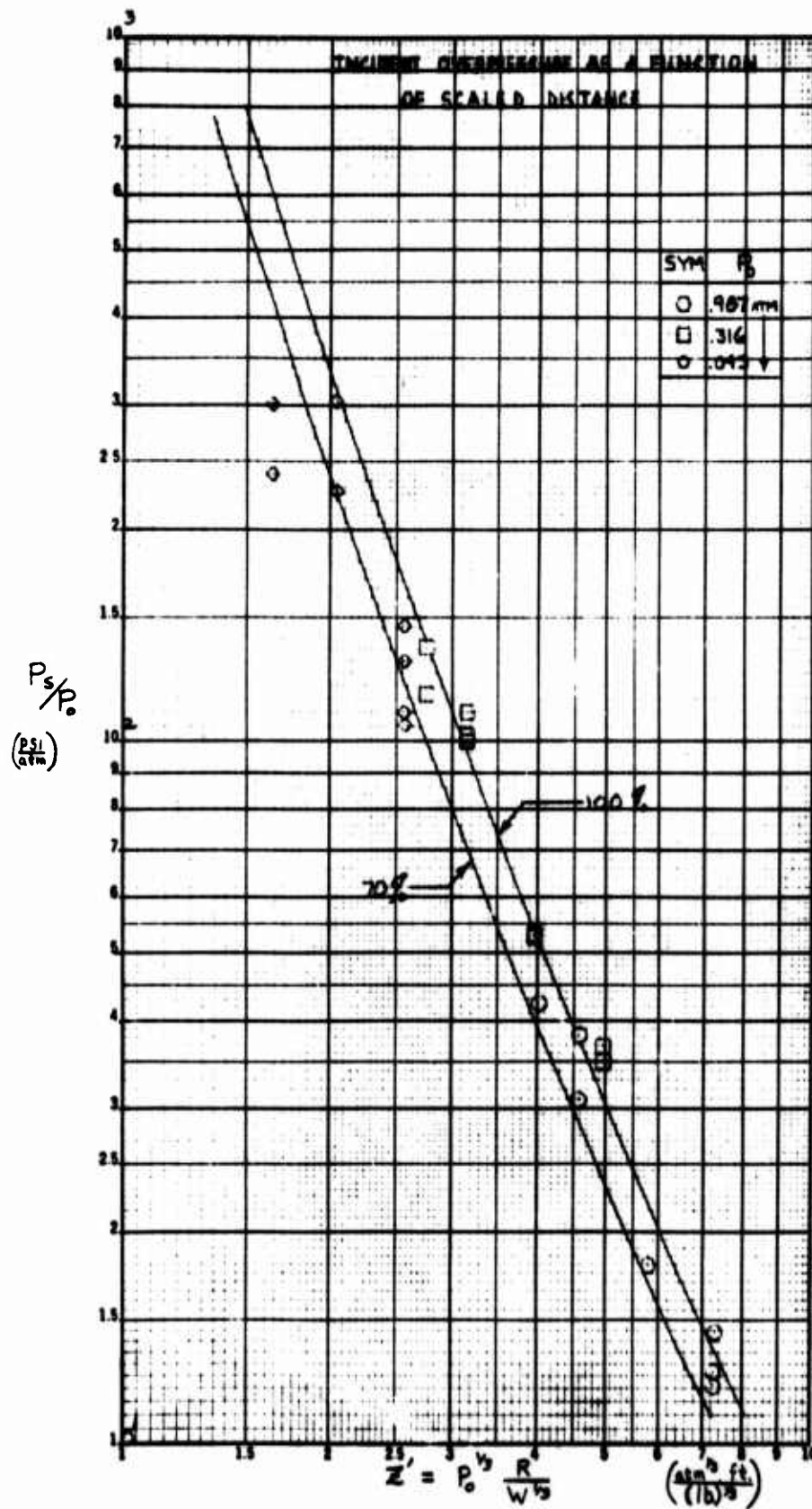


Figure 13 (a) INCIDENT OVERPRESSURE AS A FUNCTION OF SCALED DISTANCE

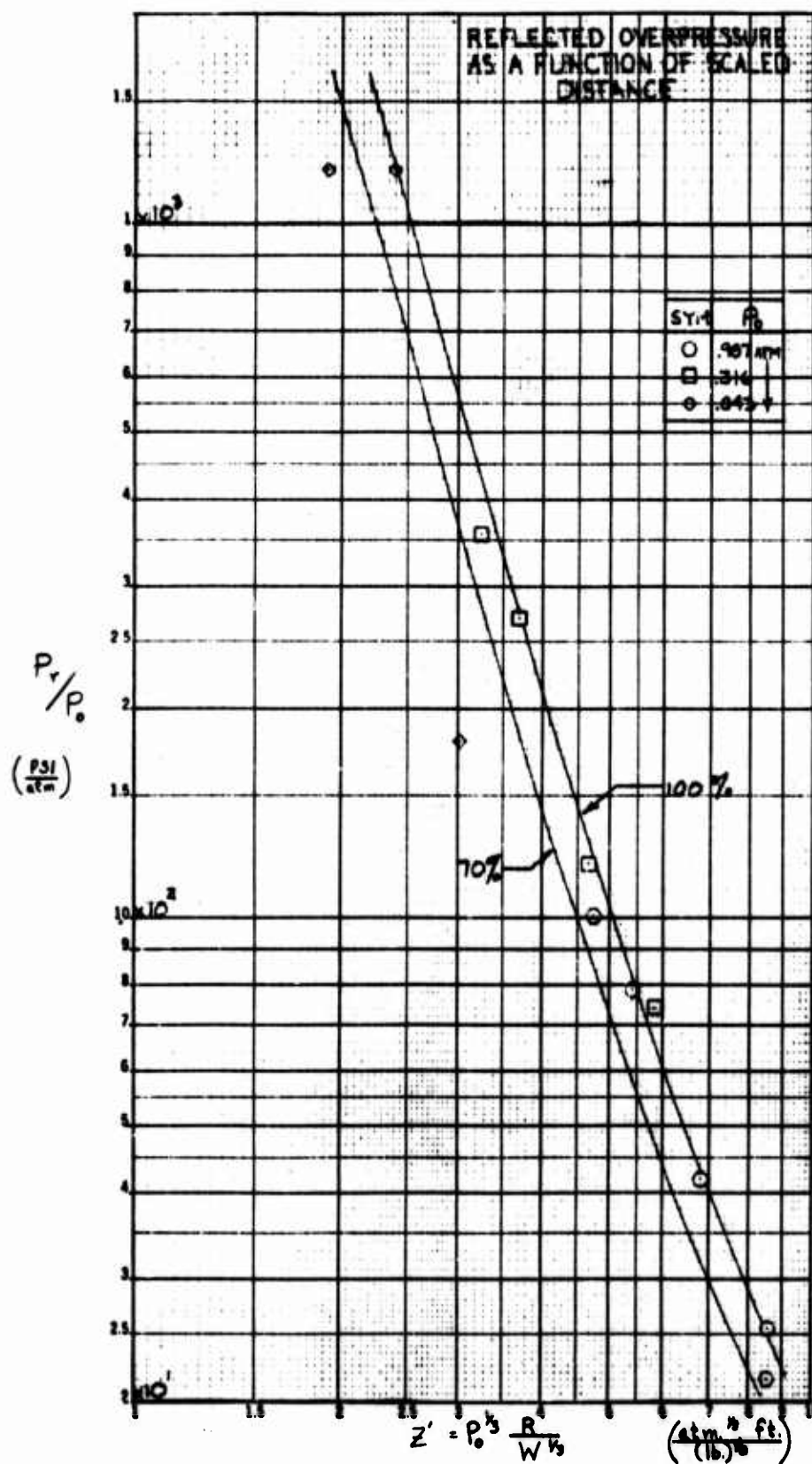


Figure 13 (b) REFLECTED OVERPRESSURE AS A FUNCTION OF SCALED DISTANCE

$\frac{I}{W}$
(mag)
(16%)

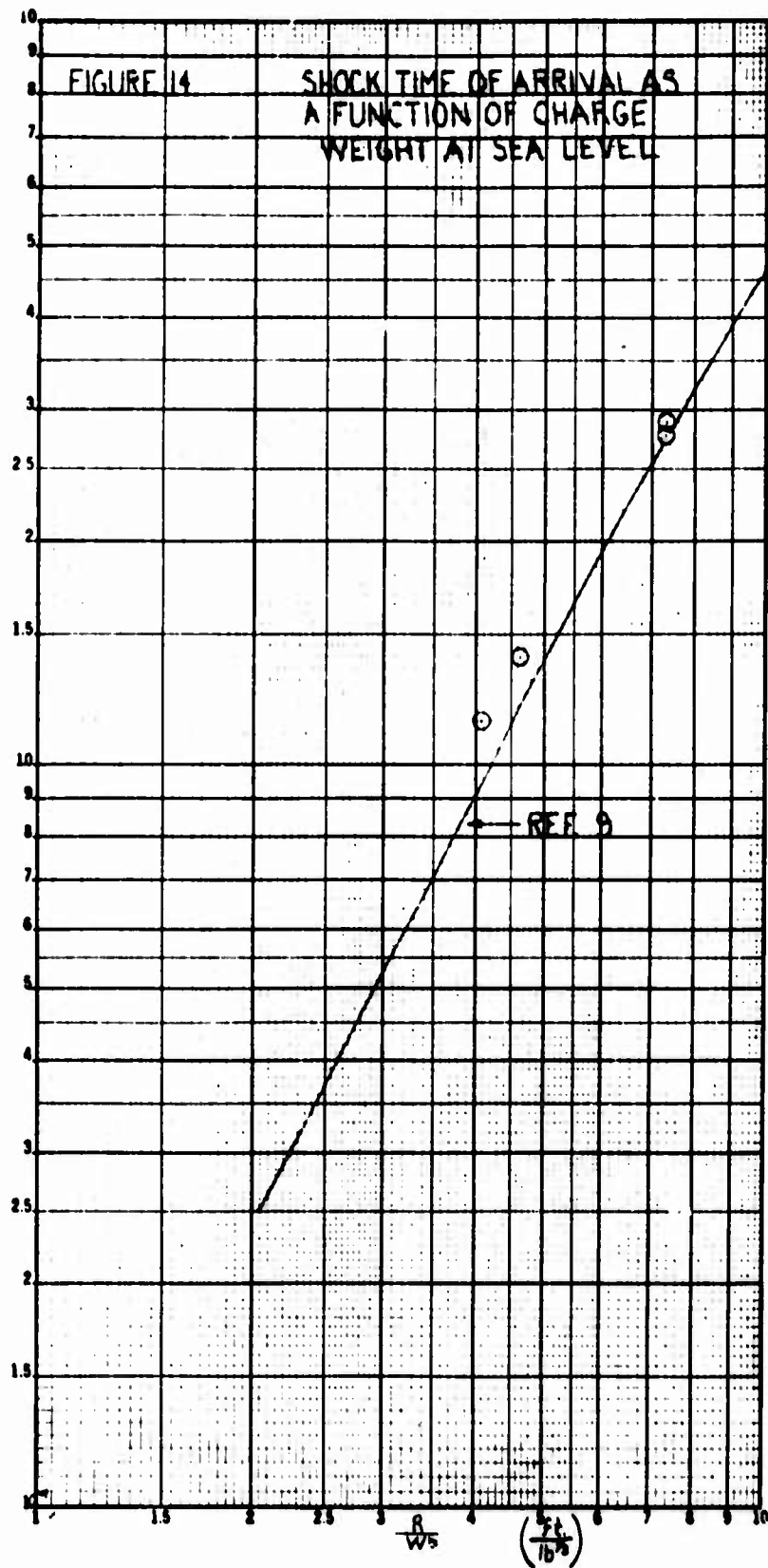


Figure 14

SHOCK TIME OF ARRIVAL AS A FUNCTION OF CHARGE WEIGHT AT SEA LEVEL

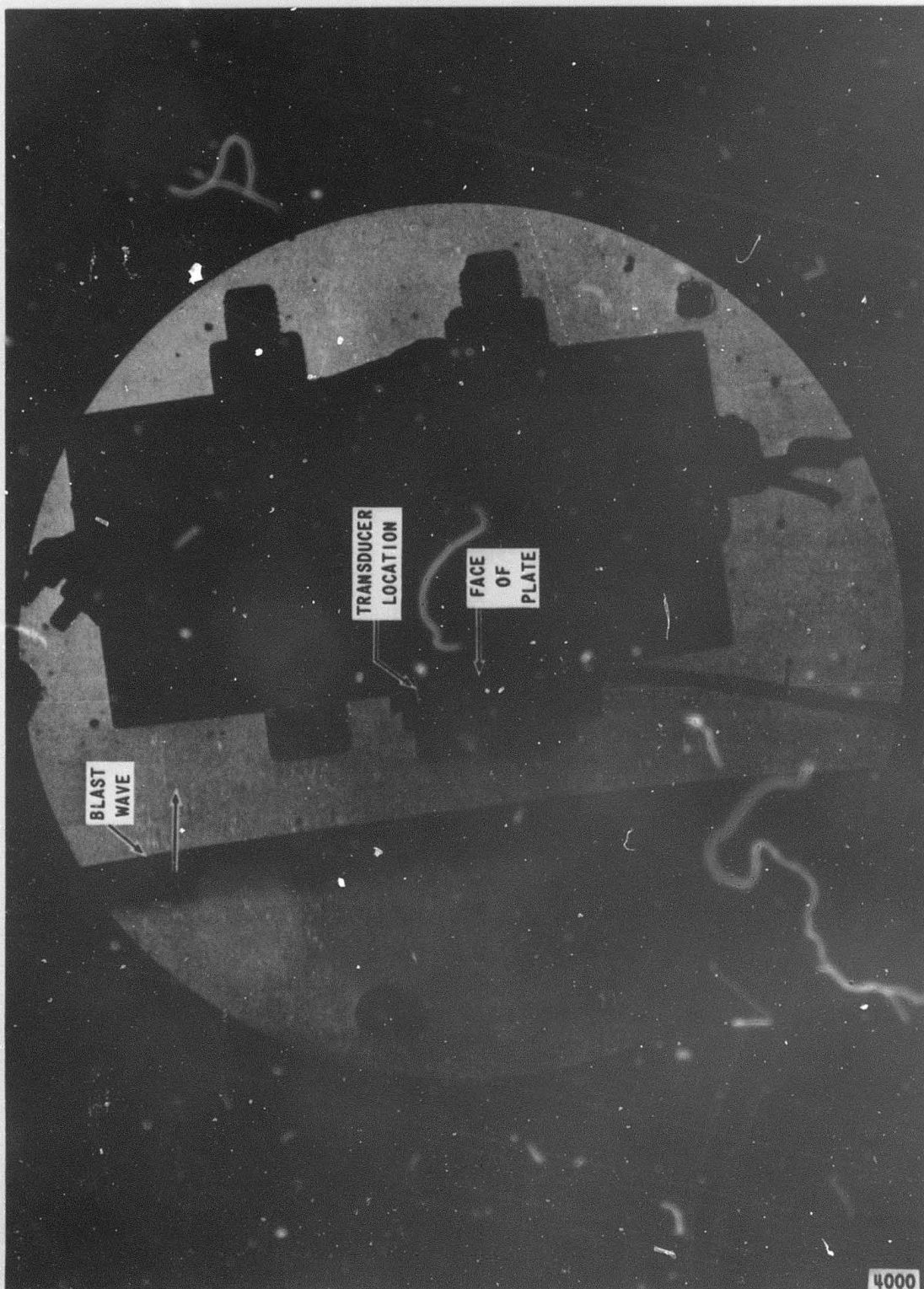


Figure 15 - SHADOWGRAPH PHOTOGRAPH OF CONE-CALIBRATION FLAT PLATE

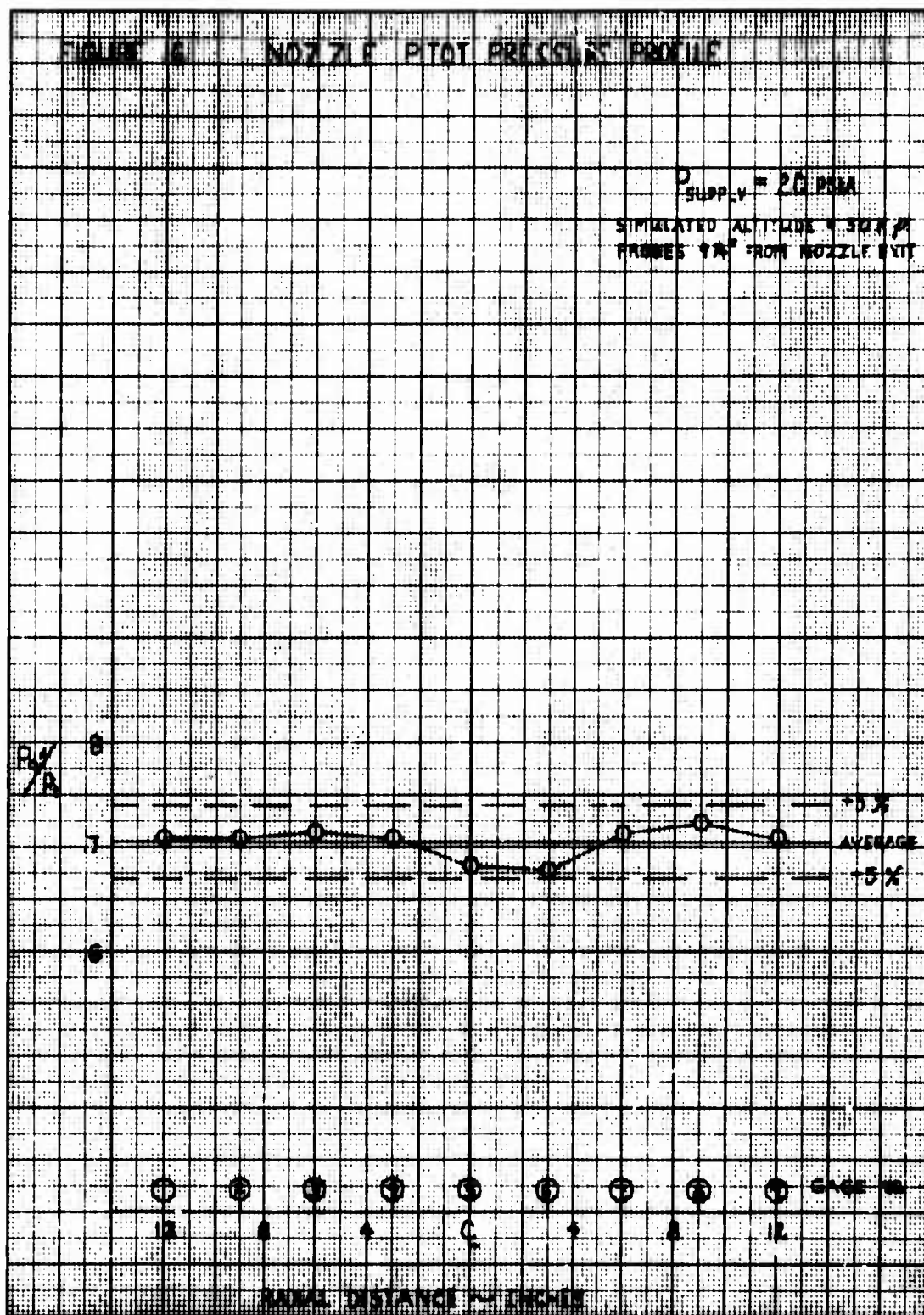


Figure 16 NOZZLE PITOT PRESSURE PROFILE

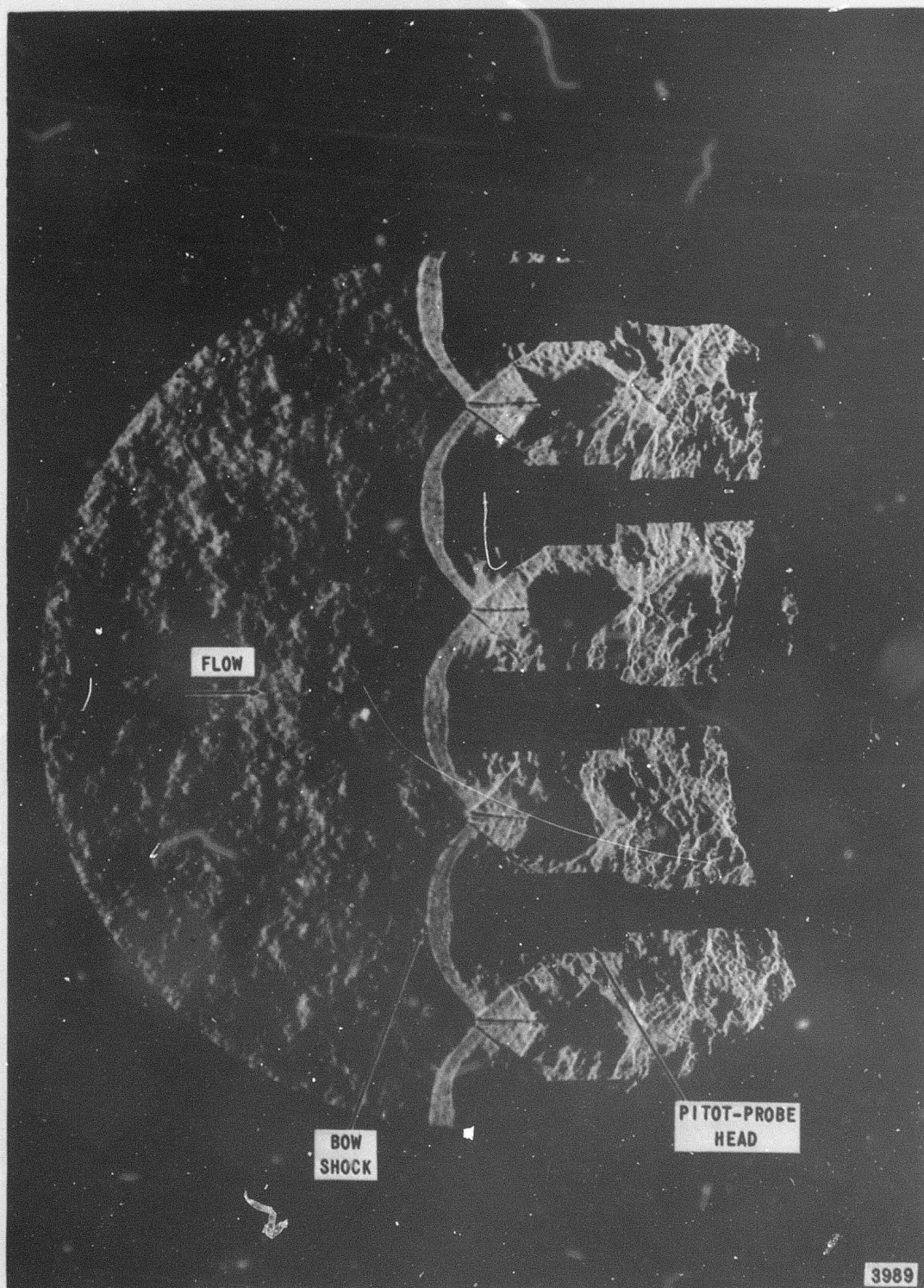
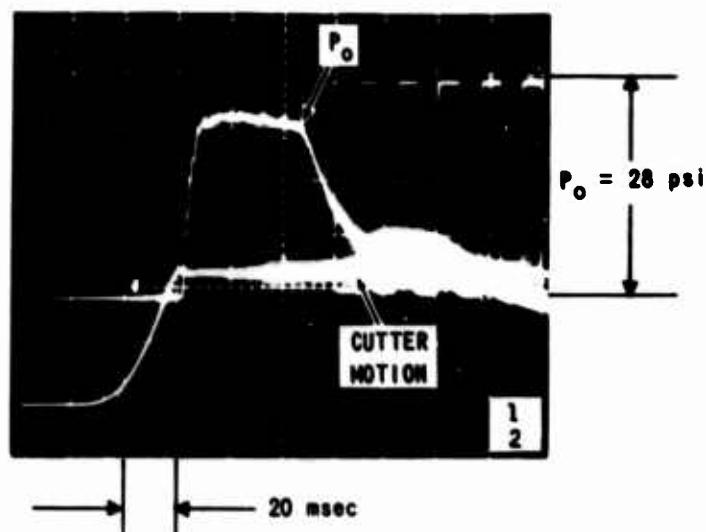
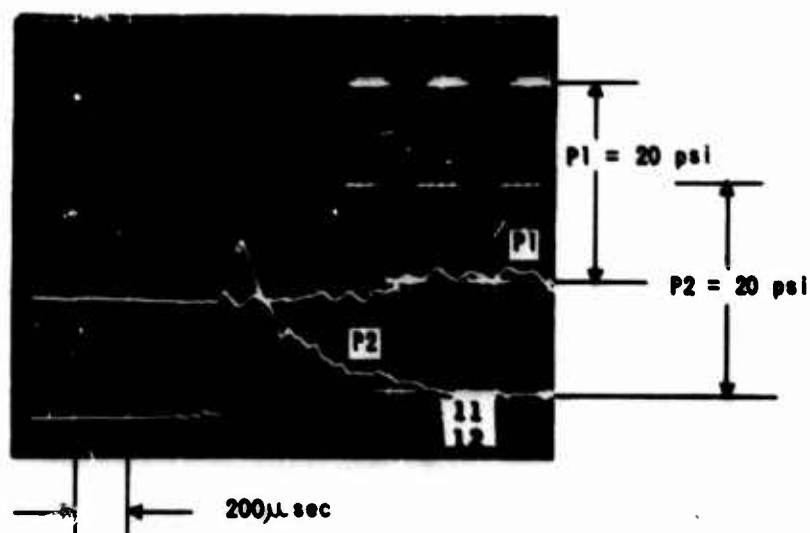


Figure 17 SCHLIEREN PHOTOGRAPH OF PITOT-SURVEY RAKE

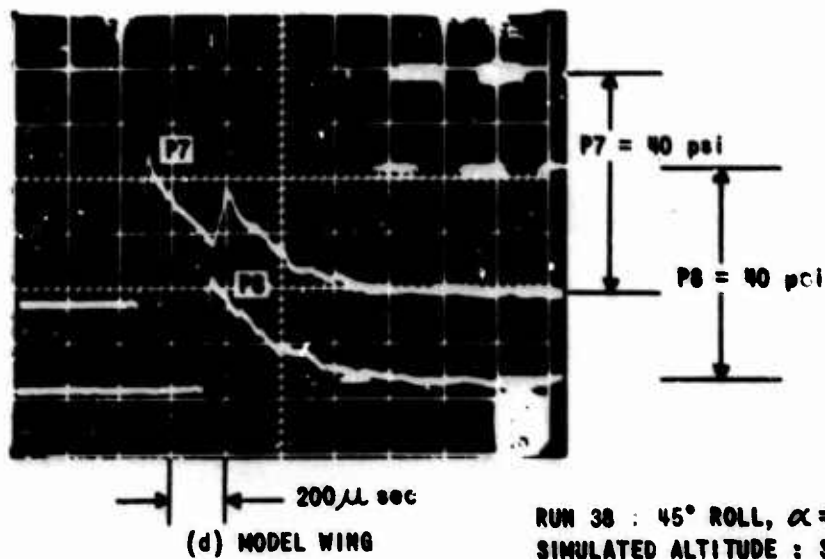
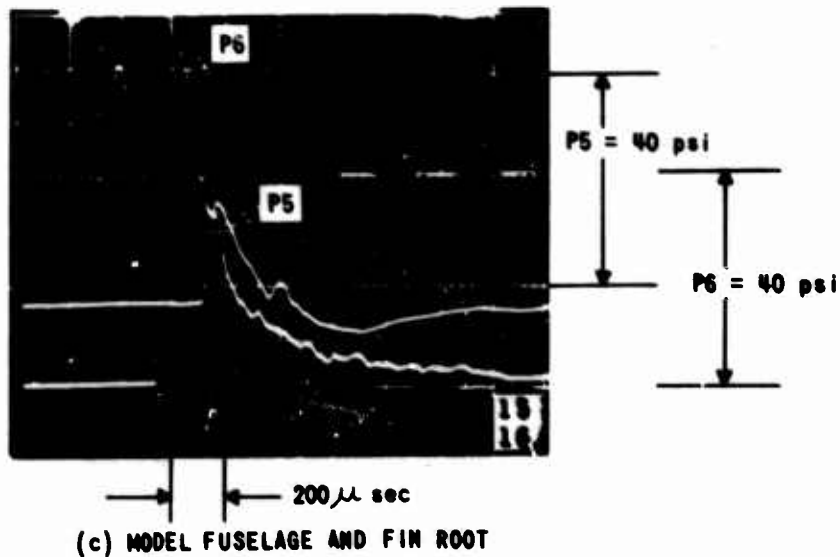


(a) EXTERNAL FLOW SYSTEM TOTAL PRESSURE (P_o)
AND DIAPHRAGM CUTTER MOTION



(b) MODEL FUSELAGE (SEE FIGURE 10 FOR TRANSDUCER POSITIONS)

Figure 18 SELECTED OSCILLOSCOPE RECORDS FOR
A MODEL RUN WITH SUPERSONIC FLOW AND
BLAST WAVE



RUN 38 : 45° ROLL, $\alpha = 0^\circ$
 SIMULATED ALTITUDE : 35 KFT
 CHARGE WEIGHT : 5.7 GMS

Figure 18 CONCLUDED

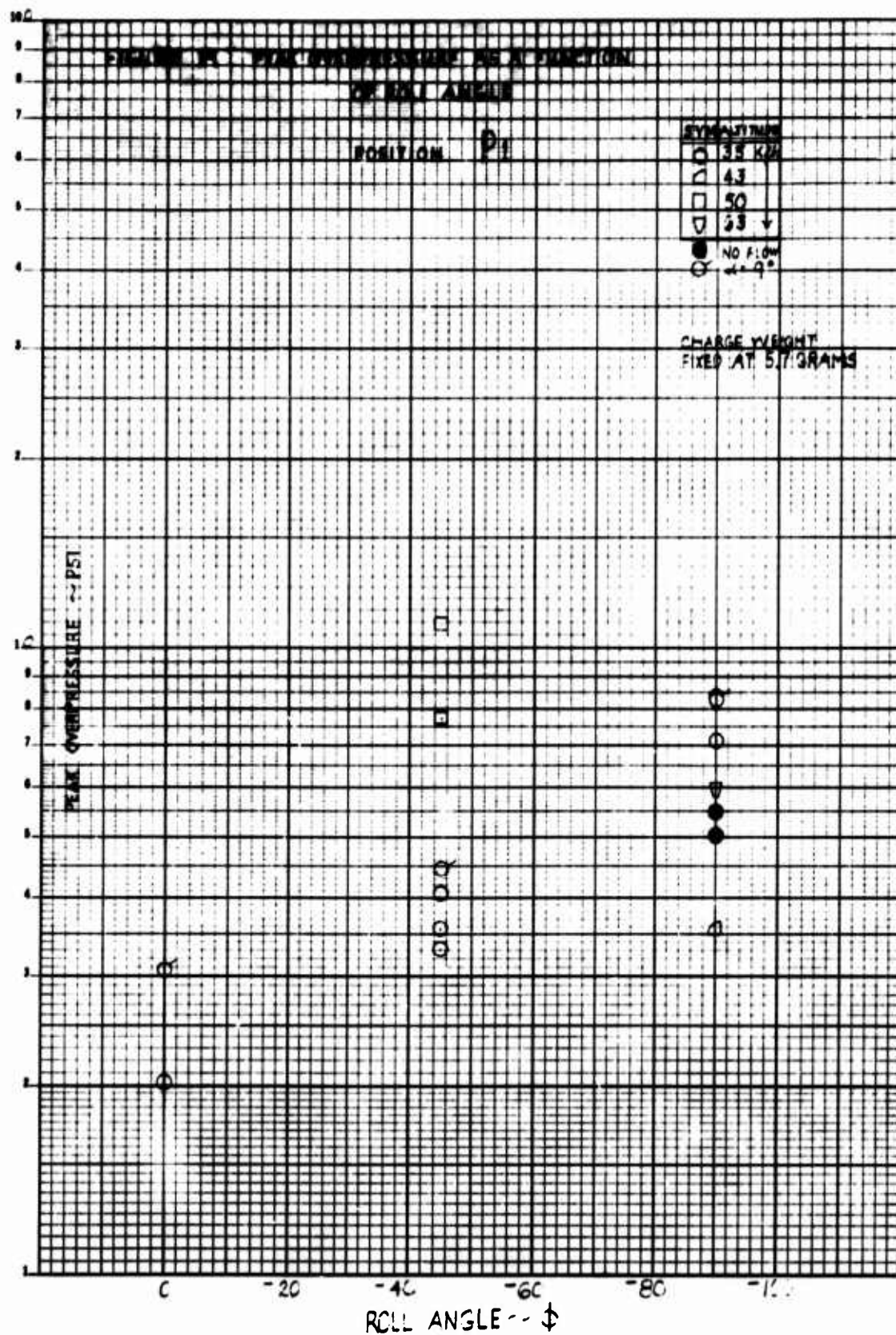


Figure 19 (a) PEAK OVERPRESSURE AS A FUNCTION OF ROLL ANGLE

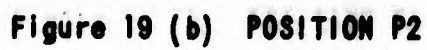


Figure 19 (b) POSITION P2

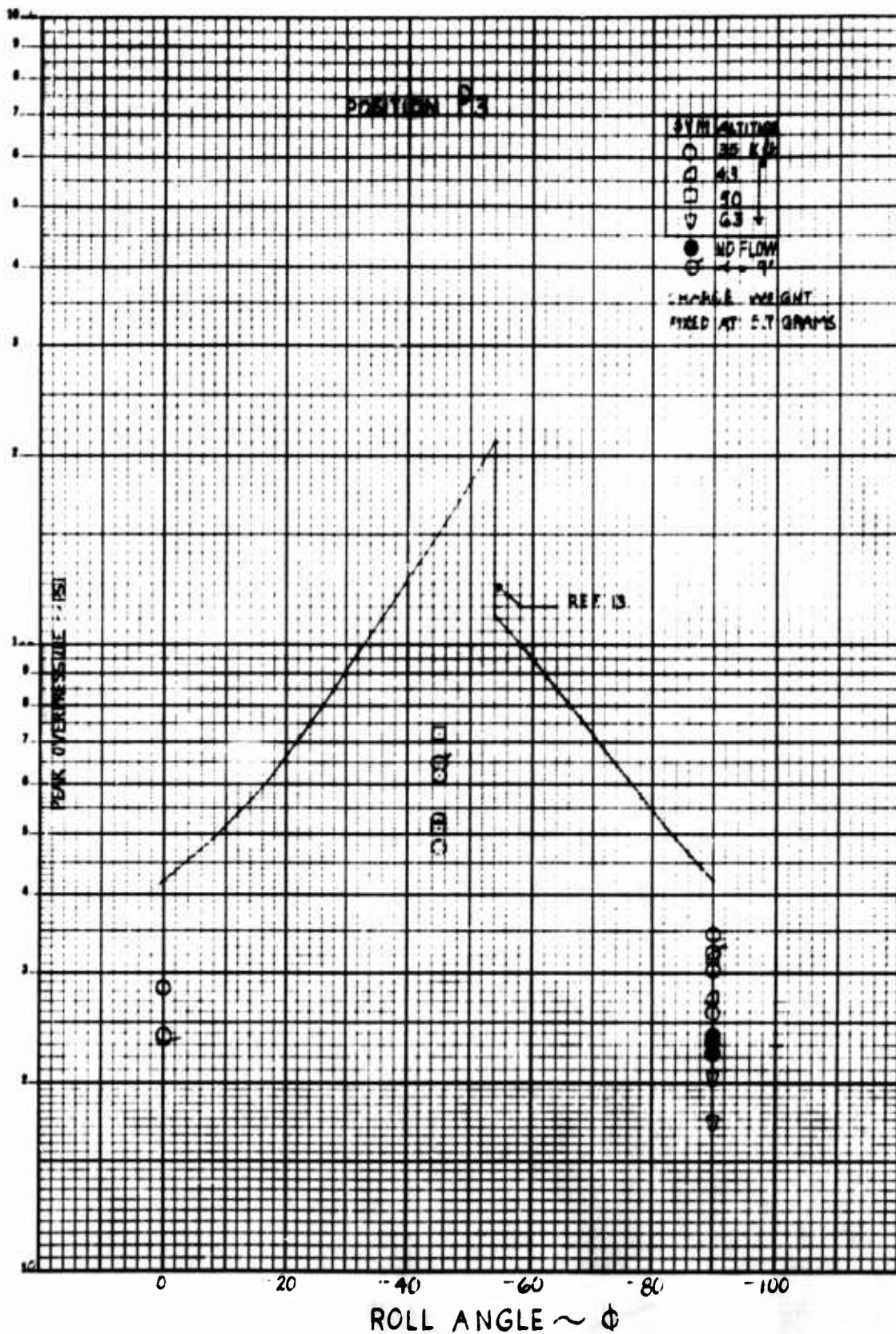


Figure 19 (c) POSITION P3

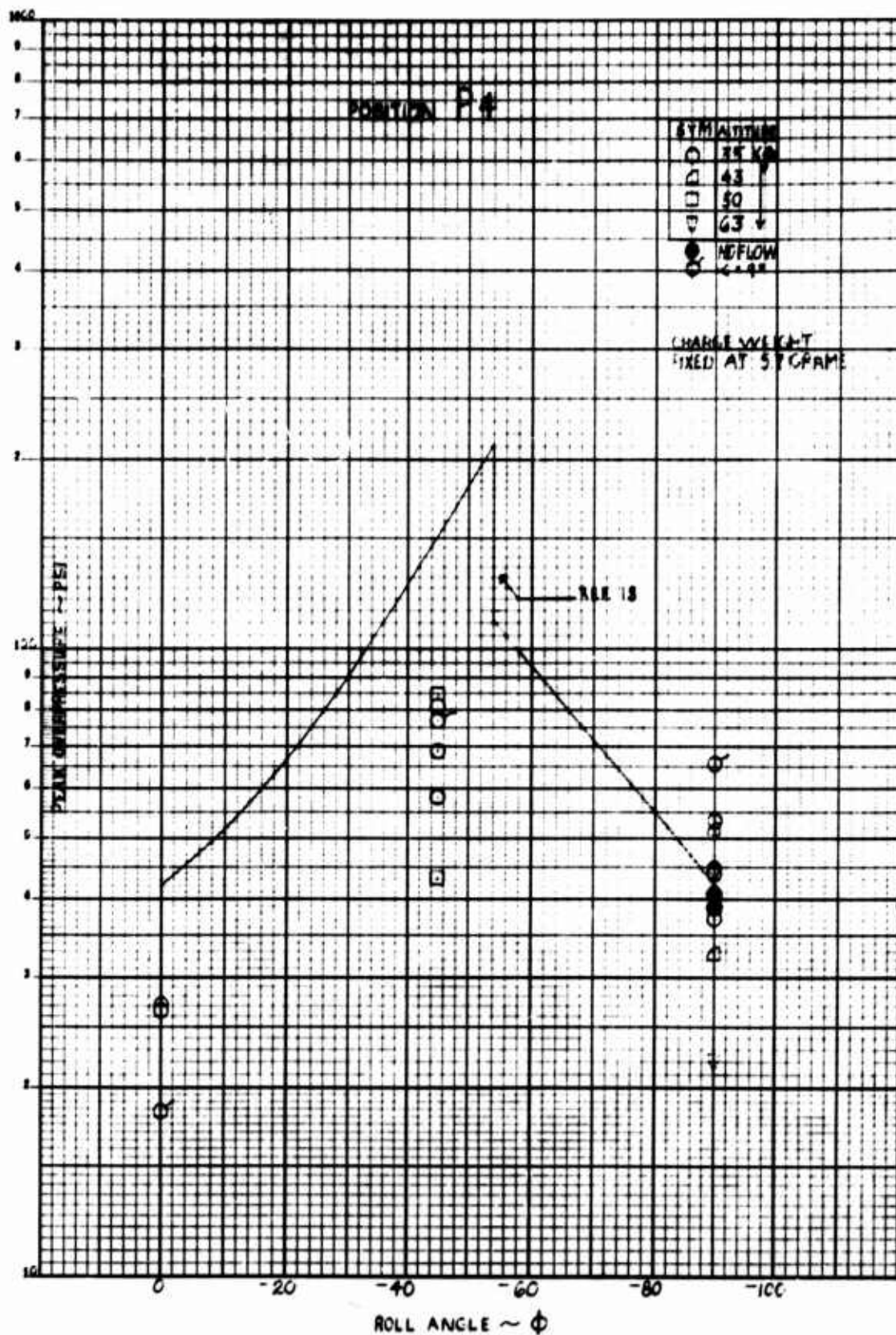


Figure 19 (d) POSITION P4

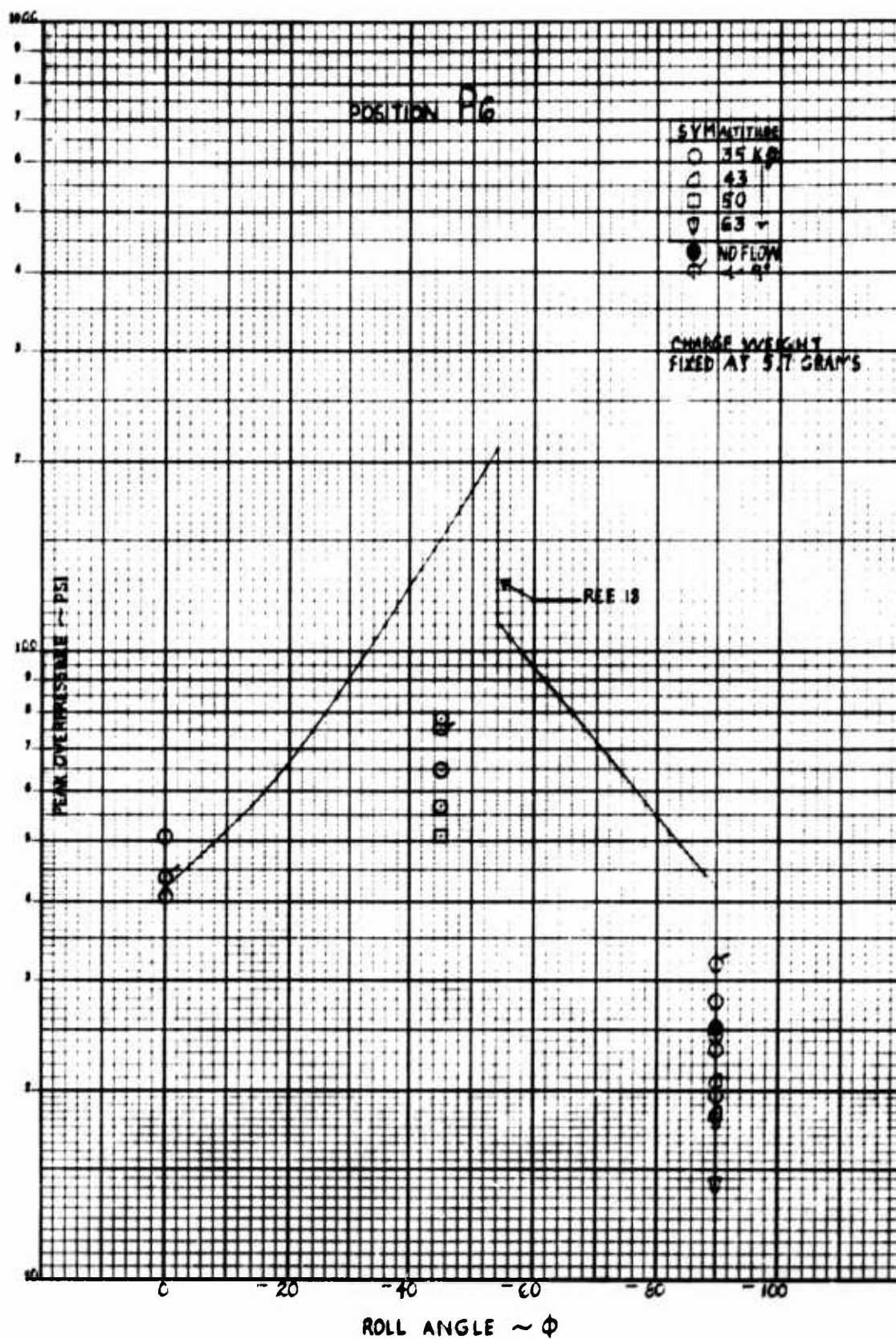


Figure 19 (f) POSITION P6

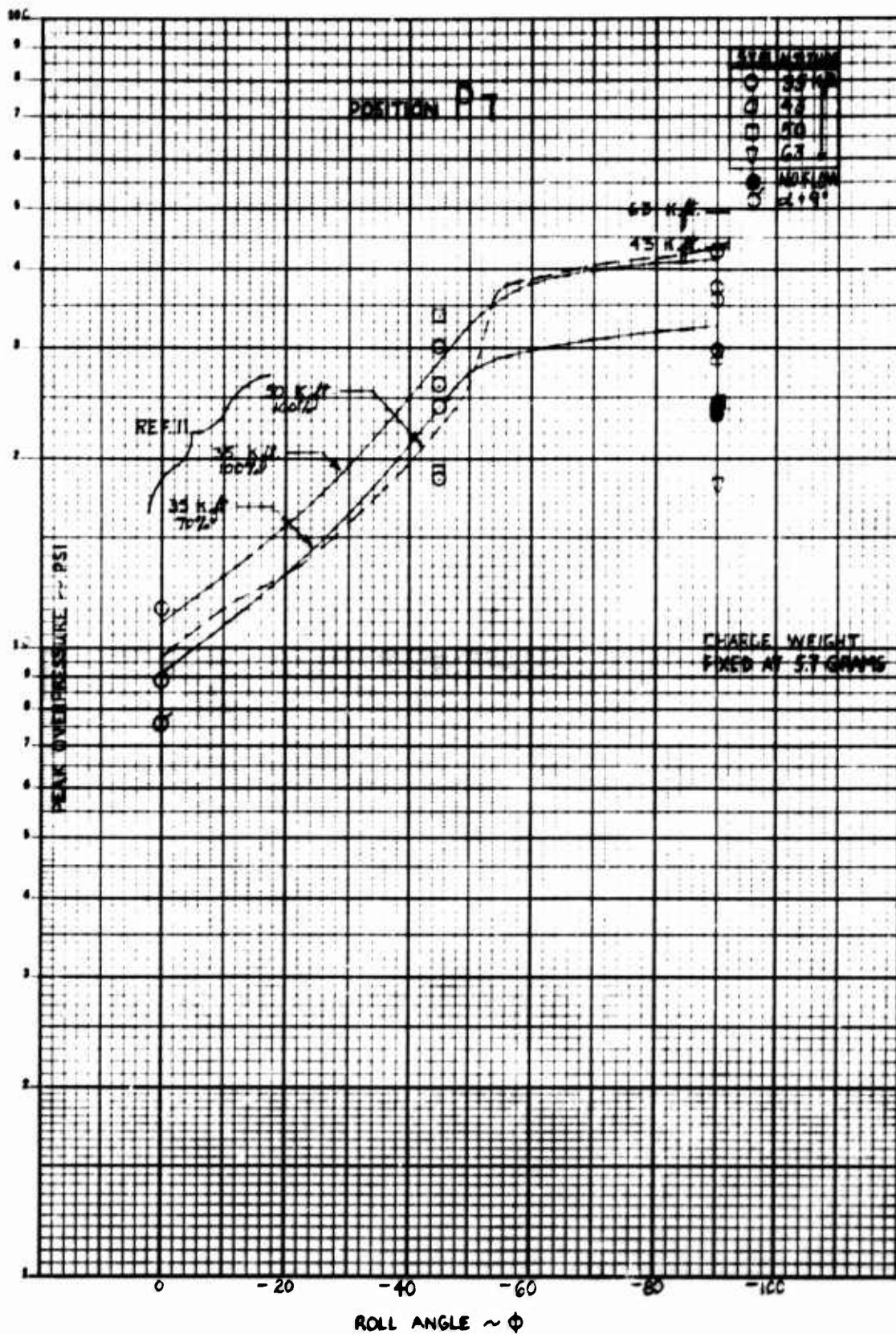


Figure 19 (g) POSITION P7

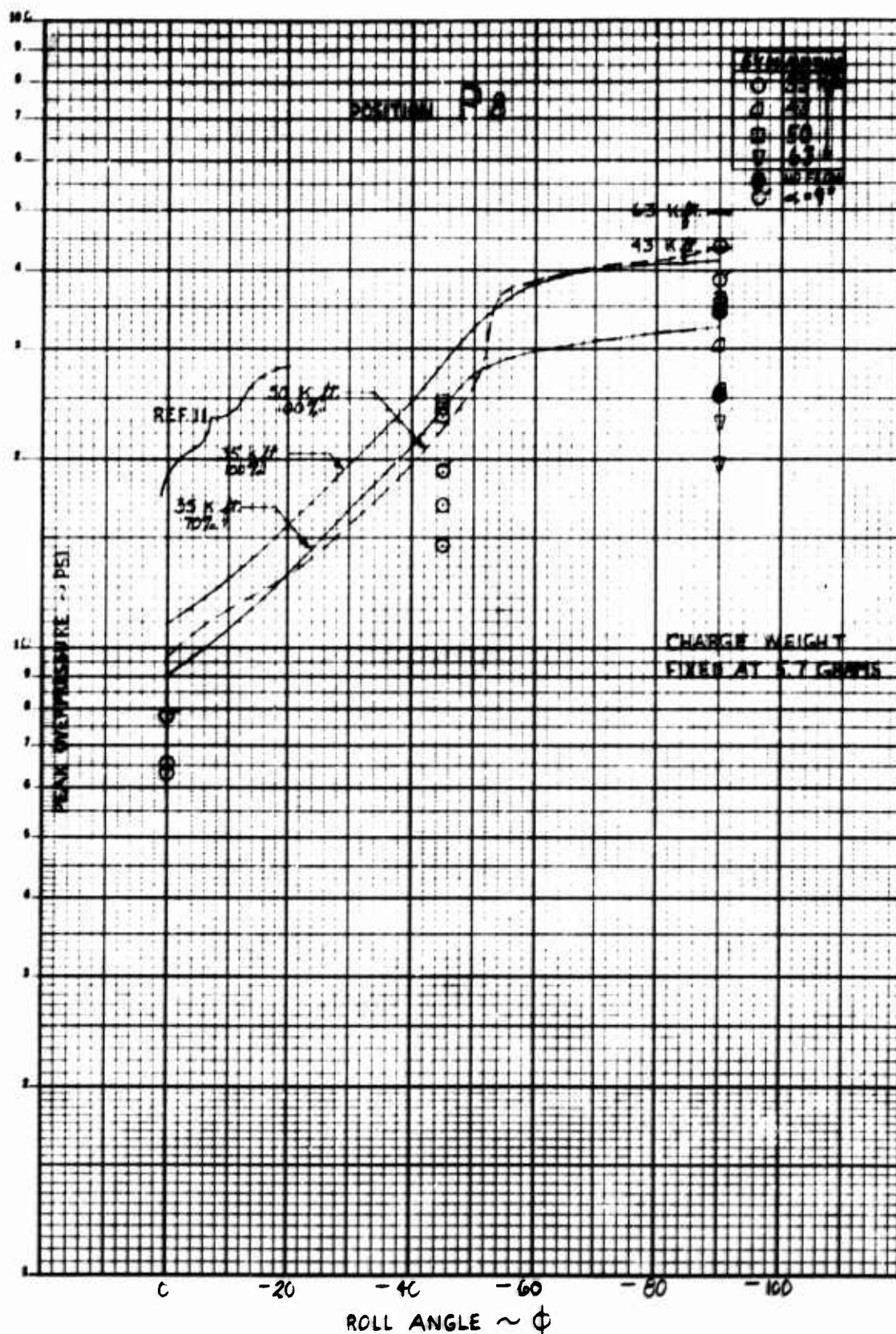


Figure 19 (h) POSITION P8

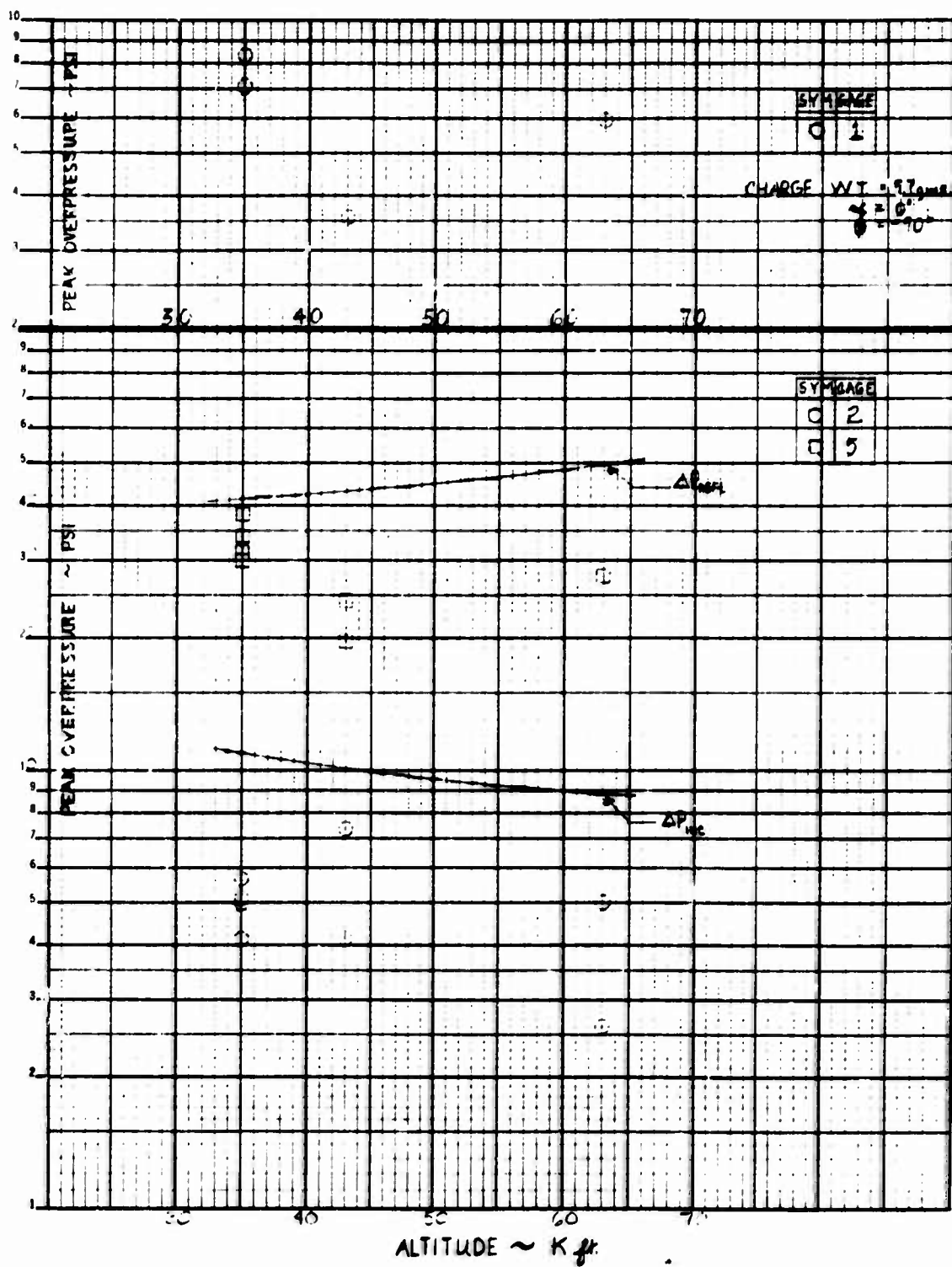


Figure 20 PEAK OVERPRESSURE AS A FUNCTION OF SIMULATED ALTITUDE

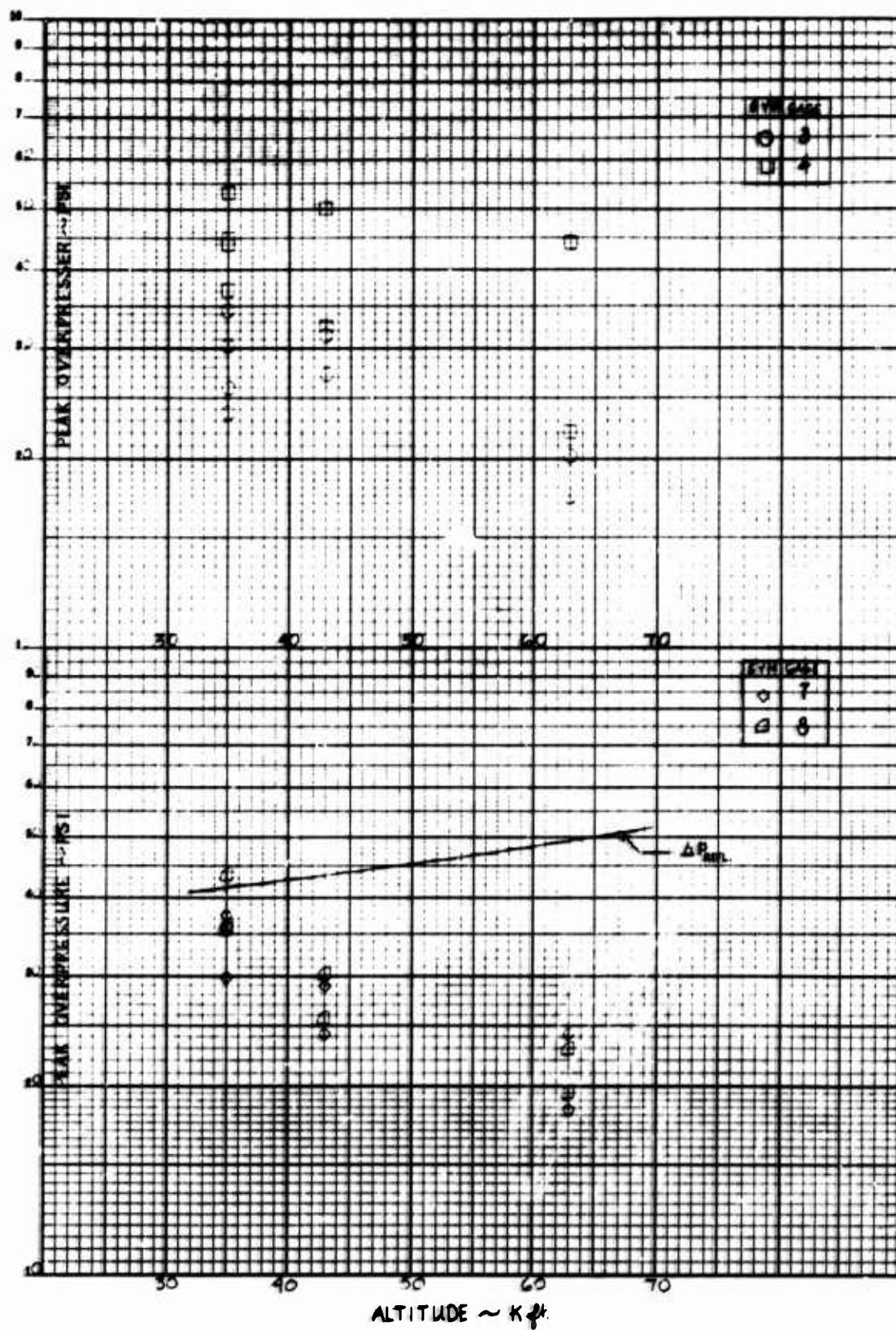


Figure 20 CONT.

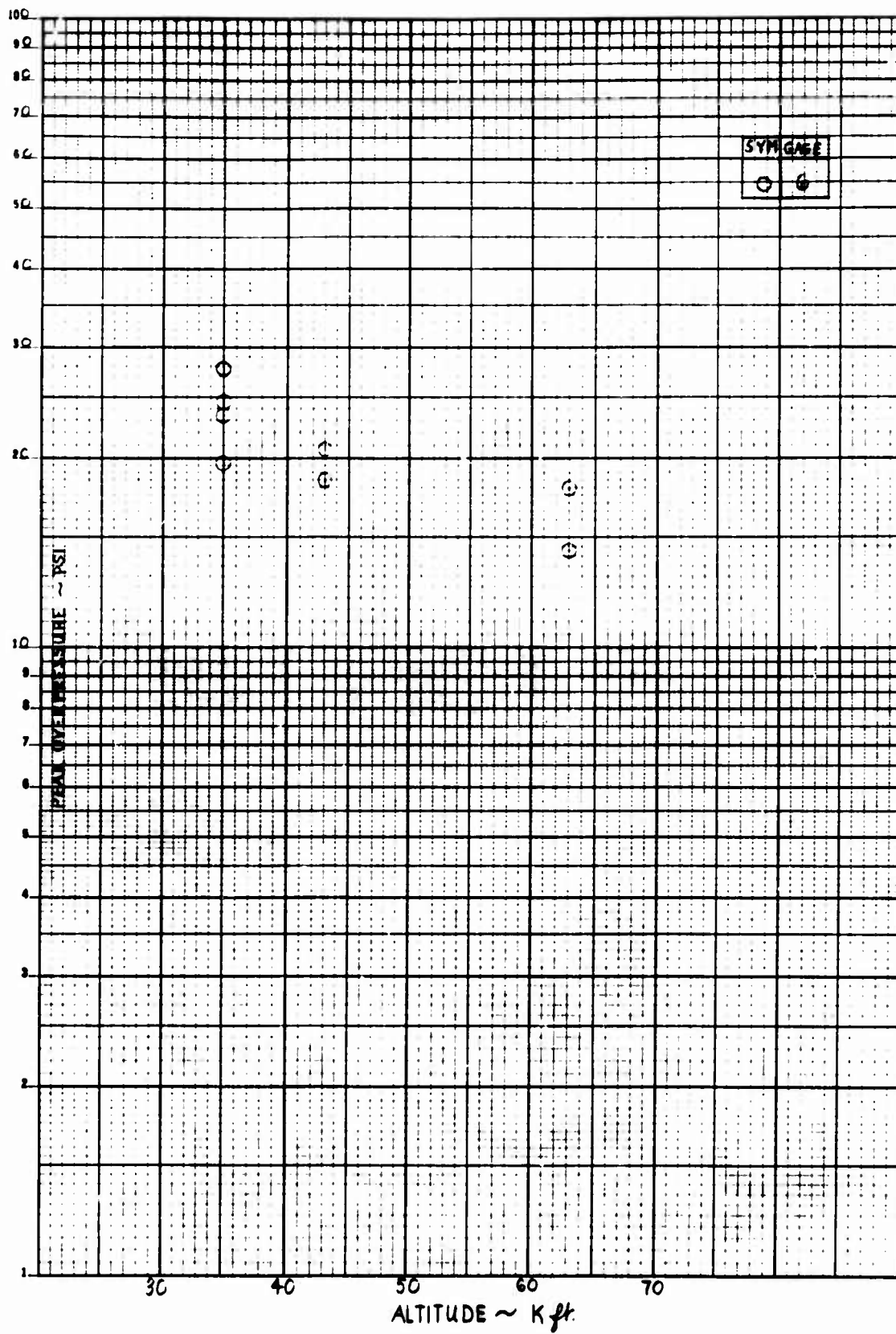


Figure 20 CONCLUDED

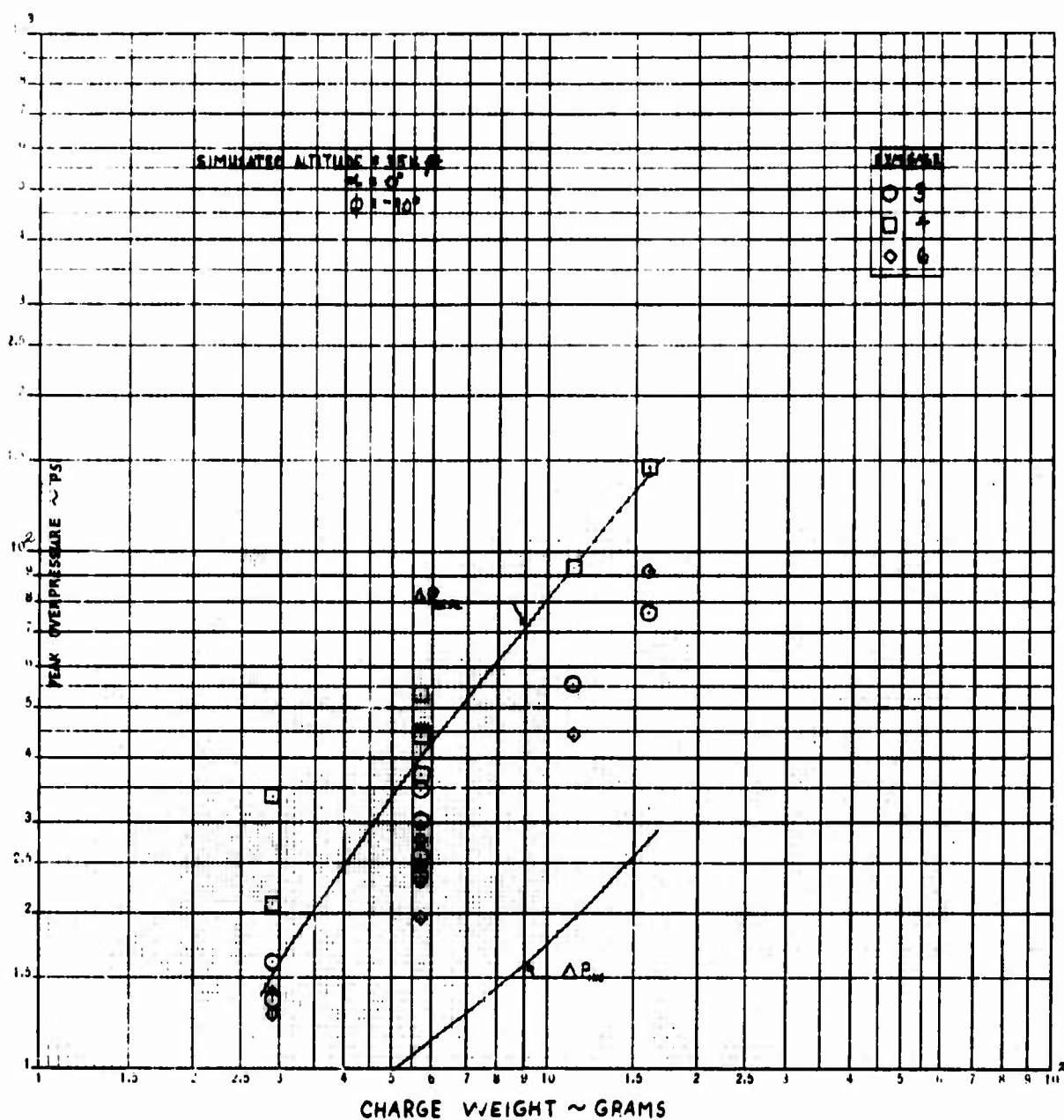


Figure 21 PEAK OVERPRESSURE AS A FUNCTION OF CHARGE WEIGHT

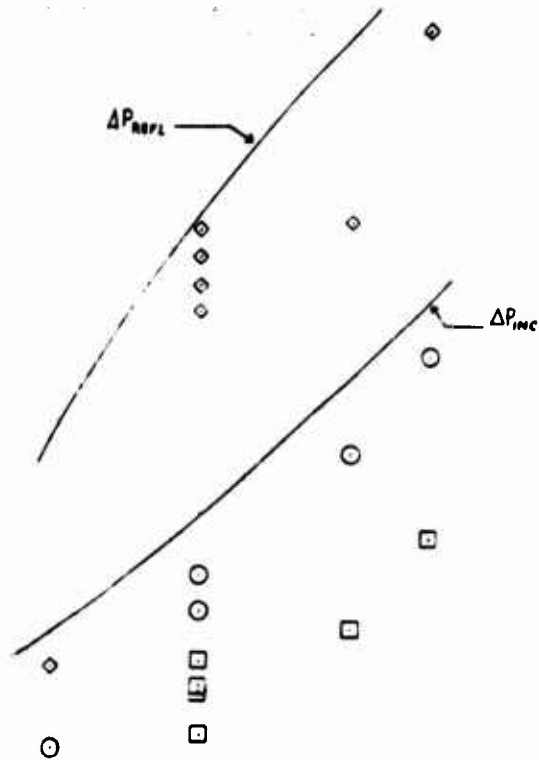
10²

10

10⁻¹

10⁻²

PEAK OVERPRESSURE ~ PSI



SYN	GAGE
○	1
□	2
◇	5

CHARGE WEIGHT ~ GRAMS

10²

Figure 21 CONT.

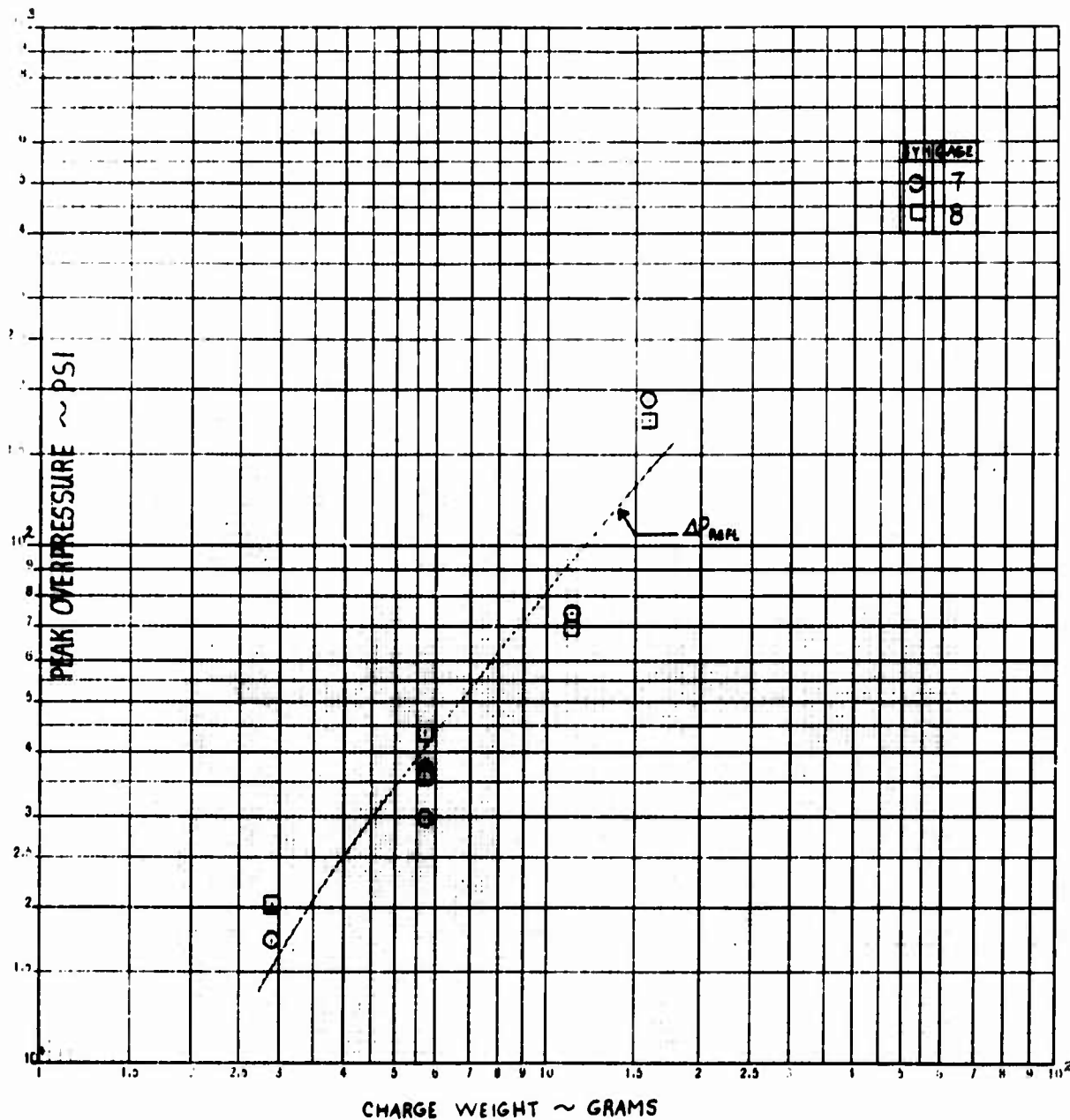


Figure 21 CONCLUDED

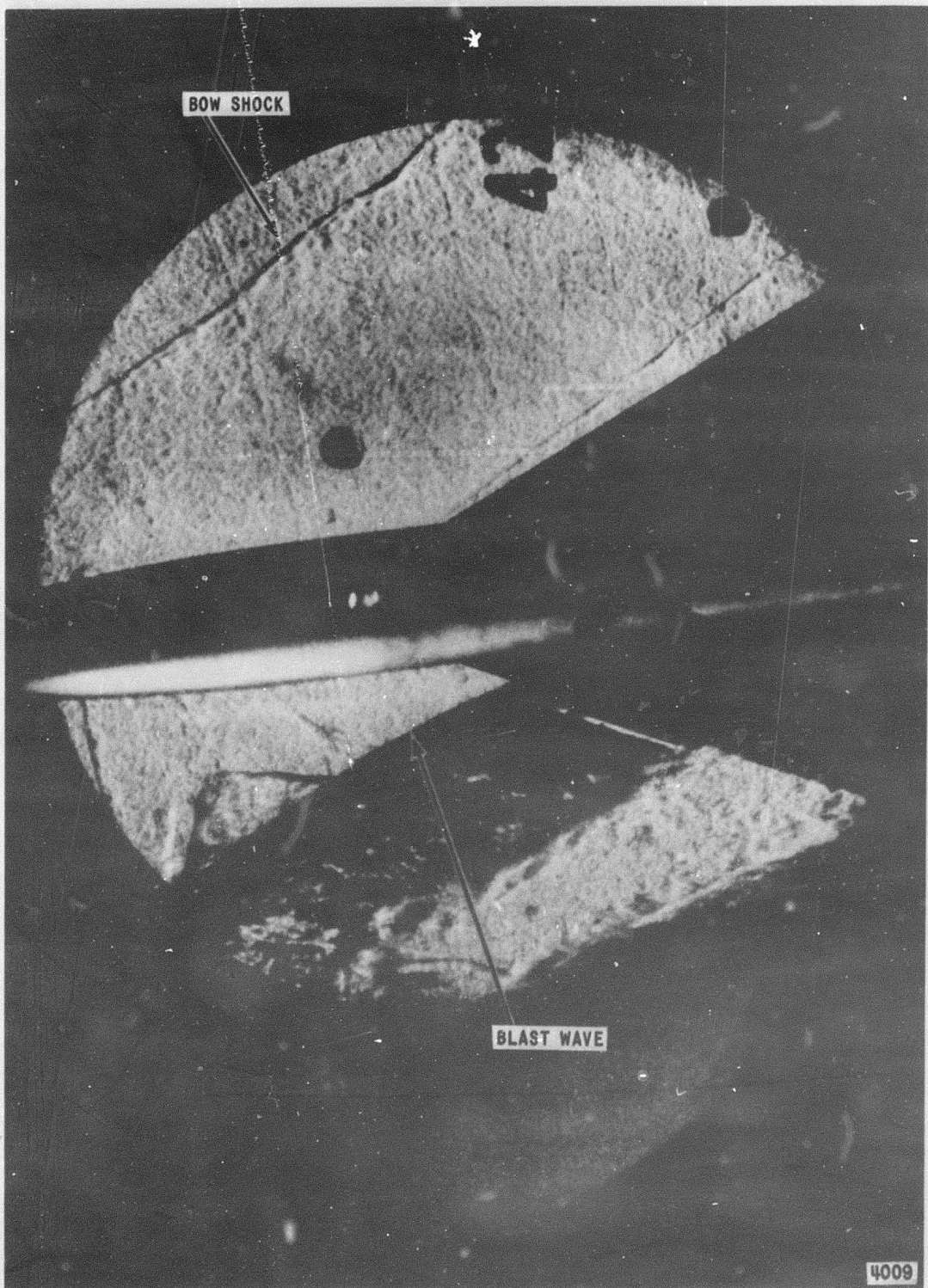


Figure 22 SHADOWGRAPH PHOTOGRAPH OF THE MODEL IN SUPERSONIC FLOW WITH BLAST WAVE

APPENDIX A

The Interpretation of Data from Instrumentation with Limited Frequency Response

Consider the case of a pressure transducer excited by a step pressure input, P . Assume also that the transducer behaves as a simple spring-mass system with light damping (actually quite a good assumption). The response of such a transducer is shown in Figure A-1 which is a plot of output against time. The transducer is excited at its natural frequency and the output is oscillatory until the damping allows it to reach its final level. If the step is semi-infinite in time, then the final level may be read with ease. If the step is only of short-duration, then techniques exist which make it possible to estimate the final, asymptotic value. If, however, the input is not a step but is a complex one containing frequencies of the same order as the natural frequency, then the output is too complex to be easily interpreted. Recourse is accordingly made to filtering of the signal.

Let us now present the response of the assumed transducer in the form of a plot of the log of the amplitude ratio against frequency. By analogy with other simply-damped spring-mass systems, the response may be expected to look like Figure A-2. The response of a simple double-section low-pass R-C electrical filter and the resultant transducer response after filtering are also shown. If the filter's corner frequency (f_c) is sufficiently below the natural frequency (f_n)[†], then the response is dominated by the filter. That is, if the excited frequencies are sufficiently attenuated, then the system behaves as a perfect transducer* with a low-pass filter on it. This is convenient because a simple R-C low-pass filter is amenable to mathematical treatment, and its properties (such as corner frequency and slope) are calculable from the electrical properties of the elements forming it.

[†] Say, one decade lower

* One which faithfully responds to any input pressure signal.

Knowing the mathematical model of the transducer system (e. g., the Laplace transform) it now remains to describe the input signal and calculate the response of the system to it. Although we do not know, a priori, the pressure-time history expected, we can make certain assumptions as to the general form expected from blast waves. Reference A-1 has performed the response calculations for a simple-section, low-pass R-C filter acted upon by a pressure signal of the form

$$P(t) = (1 - t/t_0) e^{-t/t_0}$$

t is time and t_0 is the positive duration.

This form is generally accepted as the most accurate for spherical blast waves at large distances from the source (Reference A-2). The system response for different filter time constants, $T_2 (= R.C)$, are shown in Figure A-3, copied from Reference A-1. It is seen that the peak output recorded is less than the input overpressure (P_t), the error being a function of T_2/t_0 . One would prefer to work with a system with a small value of T_2/t_0 as this gives the smallest error.

It is fortuitous that the response of such a system is more effected by the initial slope of the input than the subsequent curve. This makes it practical to analyze the response of a double, or even triple, section R-C filter to the rather simpler case of a pressure-time history of the form

$$P(t) = e^{-t/t_0}$$

Such an analysis was performed and a plot of error versus "characteristic time" (t_0) constructed for each filter chosen. This plot may then be used to correct the filtered output to obtain the peak overpressure.

References

- A-1 Crocker, M. J. and Sutherland, L. C., "The Effects Upon Shock Measurements of Limited Frequency Response Instrumentation," Wyle Laboratories-Research Staff-Report, WR 65-1, Jan. 1965.
- A-2 Glasstone, S. (Ed.) THE EFFECTS OF NUCLEAR WEAPONS (Revised Edition) U. S. A. E. C., April 1962.

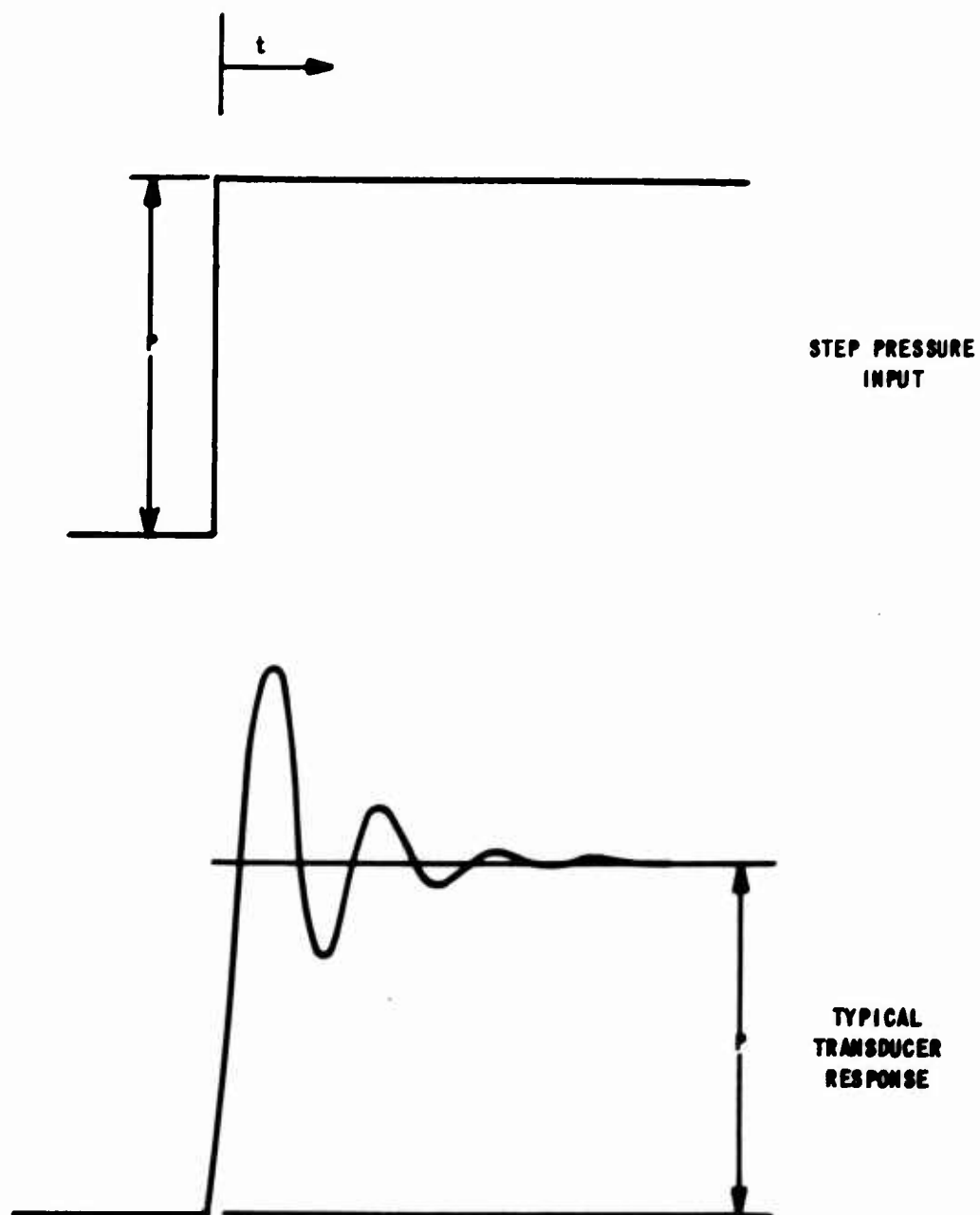


Figure A-1 RESPONSE OF A TYPICAL TRANSDUCER TO A STEP PRESSURE INPUT

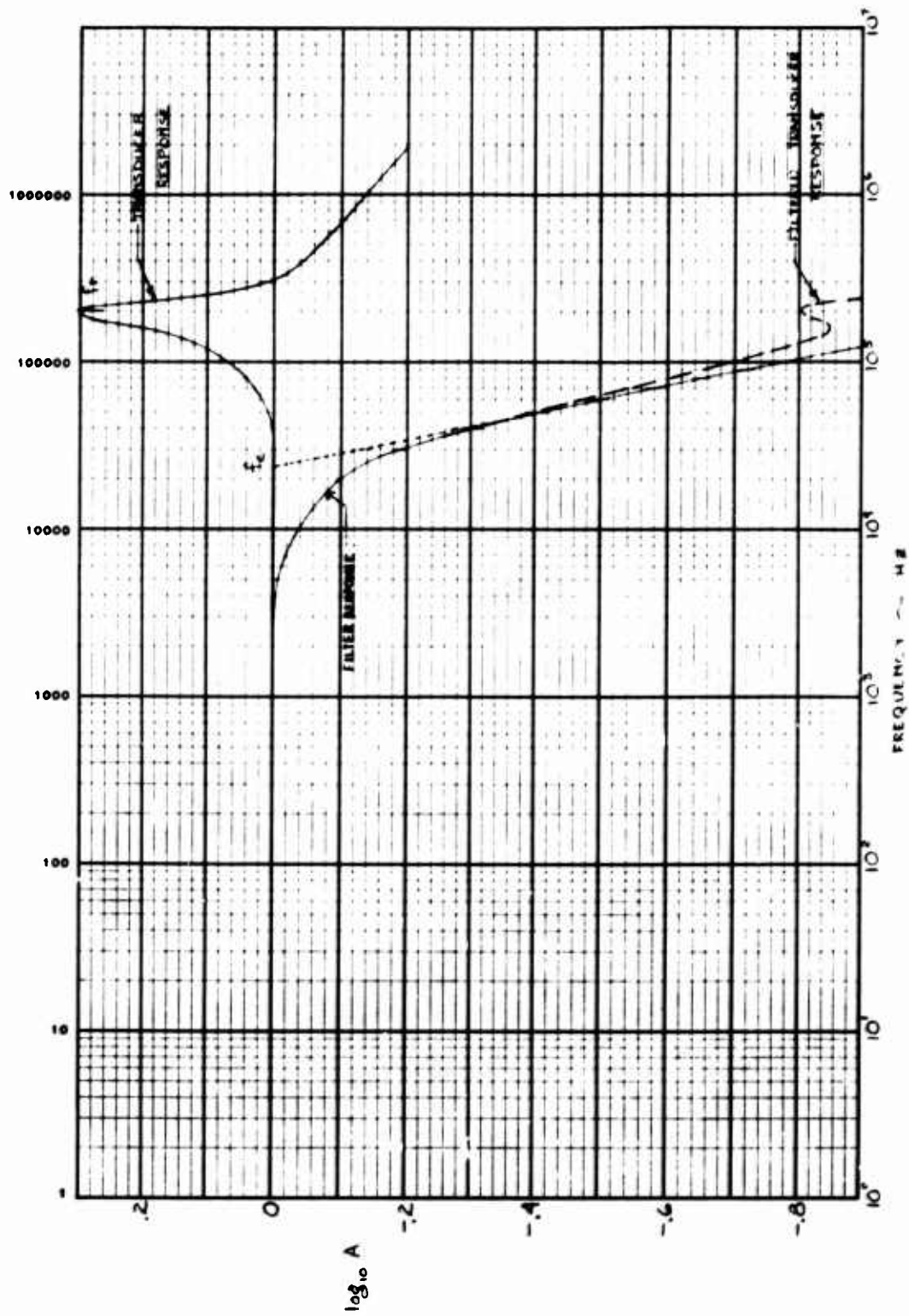


Figure A-2 RESPONSE OF A FILTERED TRANSDUCER SYSTEM

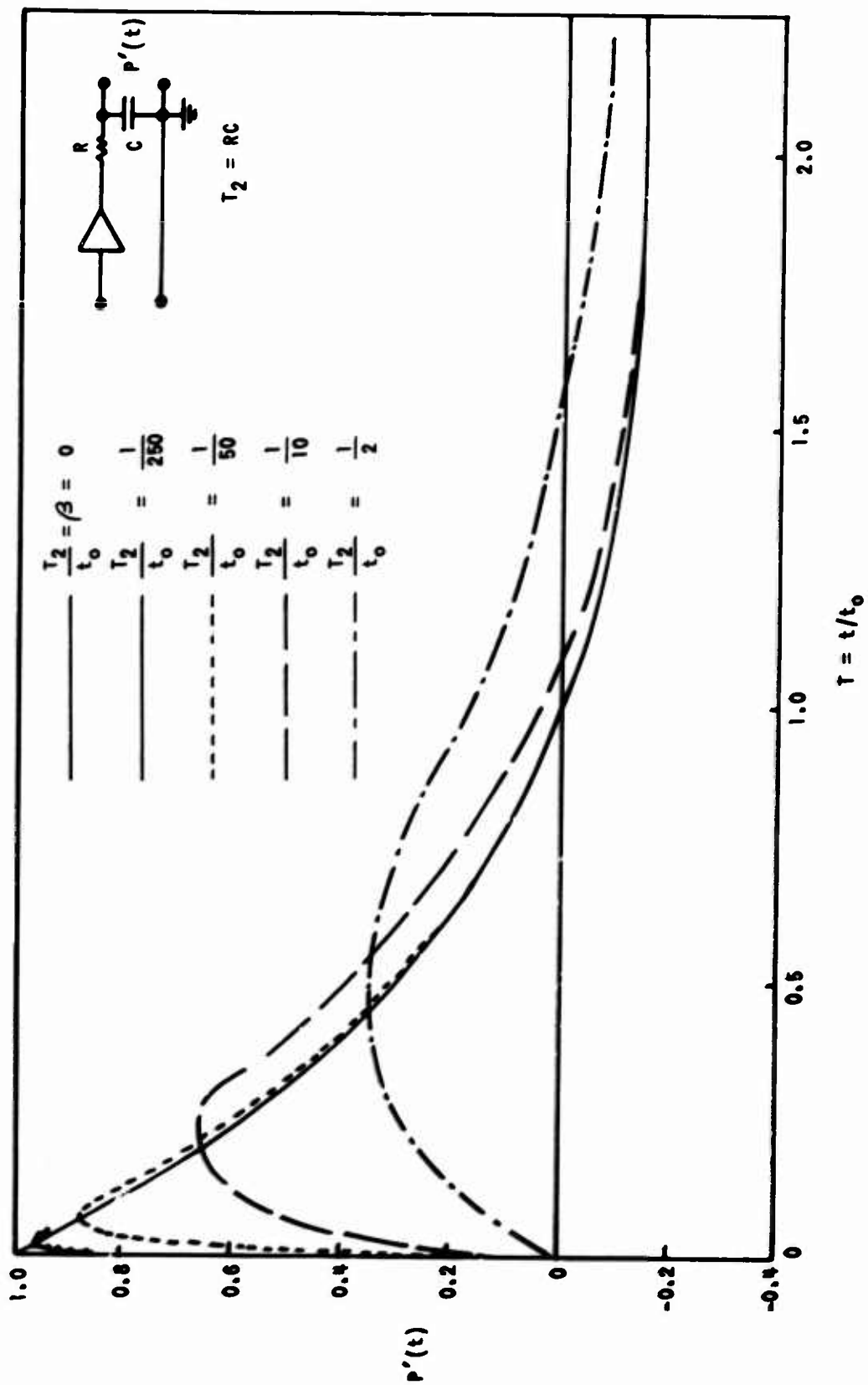


Figure A-3 EFFECTS OF SYSTEM RESPONSE, LIMITED AT HIGH FREQUENCIES,
ON IDEAL EXPLOSION PRESSURE-TIME HISTORY

APPENDIX B

Shock Tube Tests of Transducers Used in the Blast Wave Program

In order to evaluate the response characteristics of the transducers to be employed, every transducer was tested in a small shock tube. The shock tube was driven with unheated compressed air, the driven gas always being one atmosphere of room air. The shock tube had a driver length of 10' 3" and a driven length of 23' 2", the internal diameter being 2-3/4 inches. The shock tube provided a step pressure input of duration about 15 milliseconds. A typical unfiltered time history from a Kistler 603A transducer is shown in Figure B-1. The natural frequency may be estimated at about 170 KHz. Suitable filters were chosen semi-empirically: for example, 20 KHz and 40 KHz* double-section R-C filters were tried (Figure B-2). The 20 KHz filter was chosen in this case. In general, the highest frequency was chosen compatible with the necessity to attenuate the transducer natural frequency. It transpired that 20 KHz filters were necessary for the Kistler 603A transducers, whereas 40 KHz was adequate for the pcb-type transducers. The responses of a typical pcb transducer, both with and without filters, are presented in Figure B-3. This type of transducer was generally better than the Kistler, the resonance being less pronounced and at a higher frequency (about 300 KHz in the example shown).

The shock tube was also used to evaluate mounting techniques for the transducer, it being necessary to develop a technique to allow transducers to be placed in the wing. The design of the mount is critical to the successful use of quartz pressure transducers for fast response measurements: a high degree of rigidity is required. In order to insulate the transducer from the model to minimize electrical noise, Boron Nitride was chosen for the transducer mounting washer. Figure 8(b) of the report shows the transducer installation which was developed.

* 6 db down

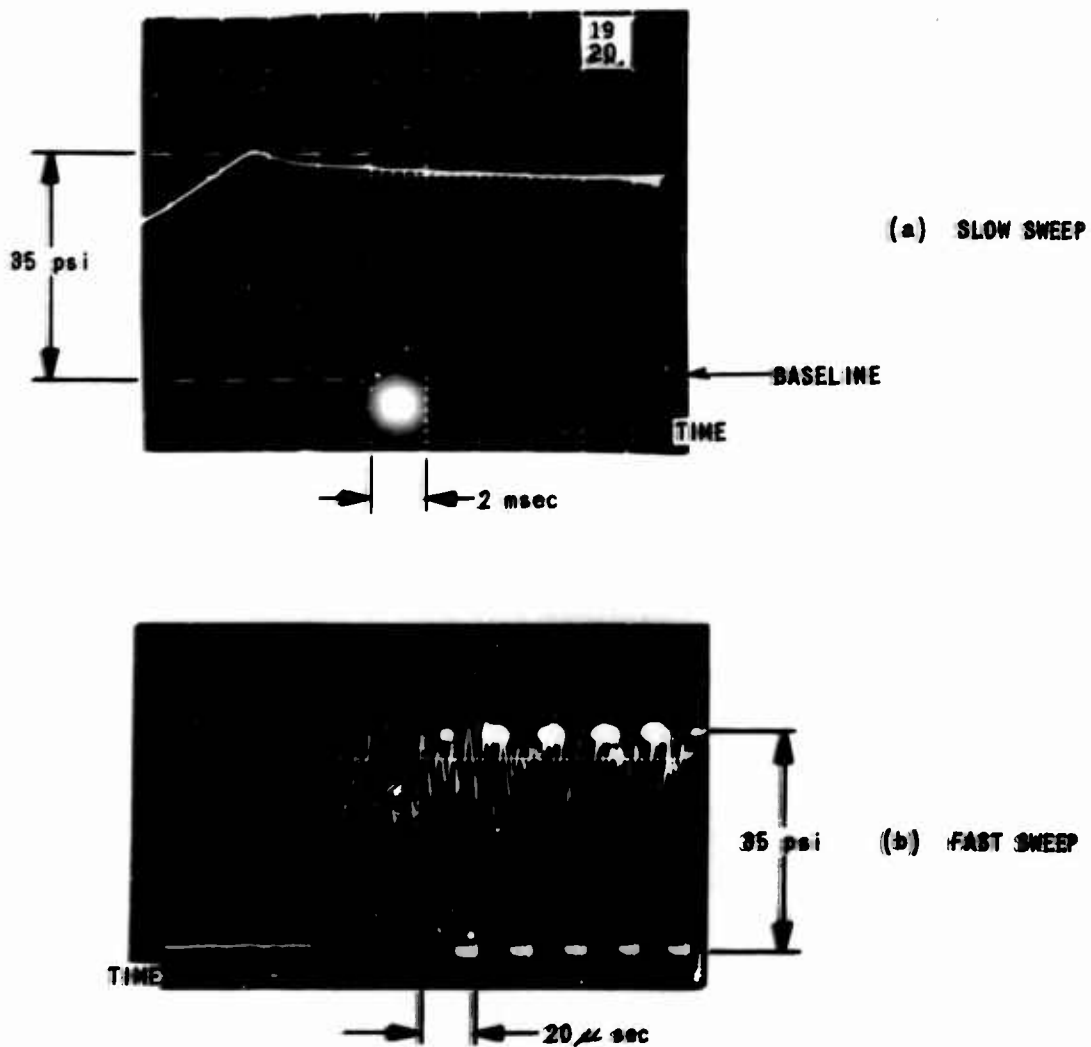


Figure B-1 UNFILTERED RESPONSE OF A KISTLER 603A TRANSDUCER
EXCITED BY A STEP PRESSURE INPUT

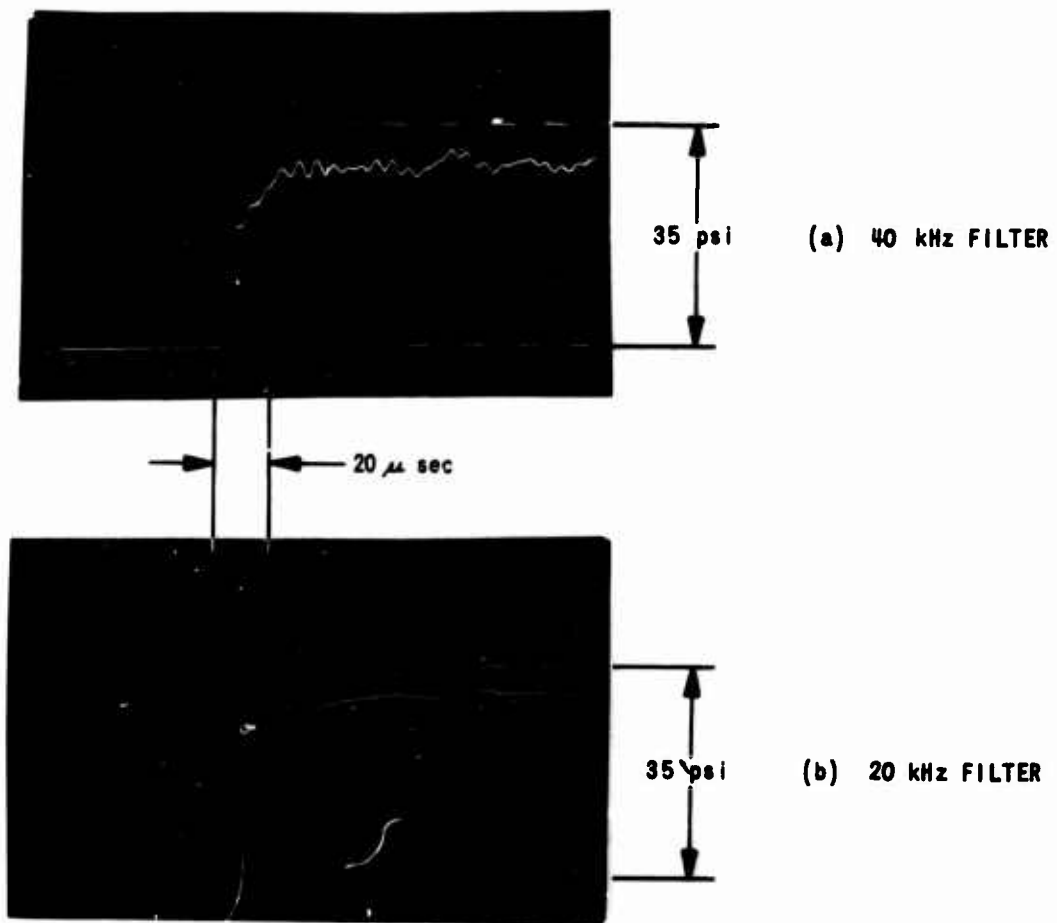
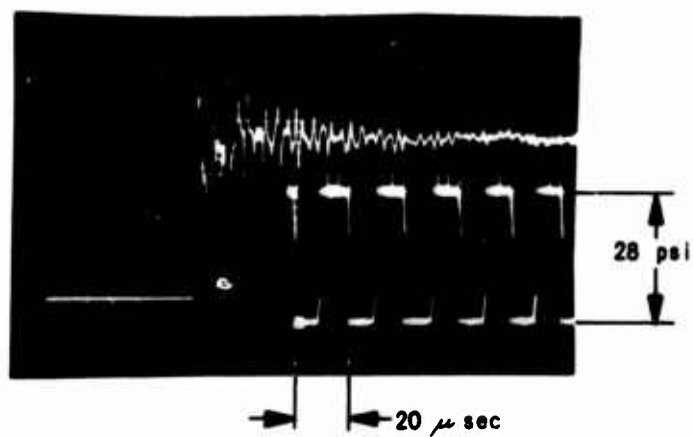
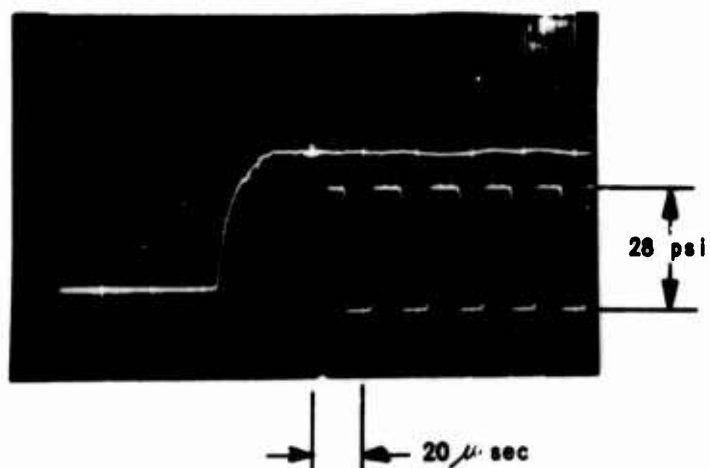


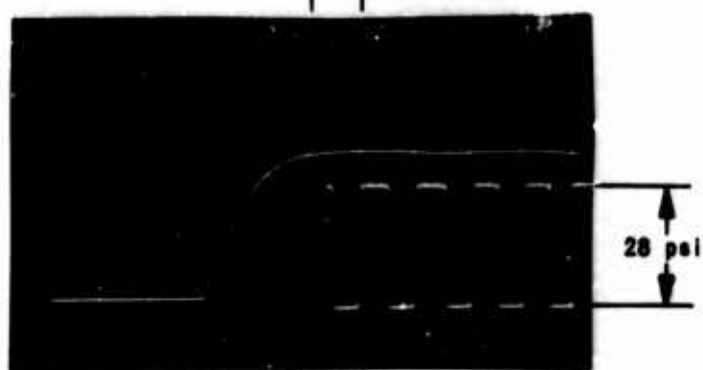
Figure B-2 KISTLER 603A TRANSDUCER RESPONSE WITH LOW-PASS RC FILTERS



(a) UNFILTERED



(b) 40 kHz FILTER



(c) 20 kHz FILTER

Figure B-3 RESPONSES OF A pcb TYPE TRANSDUCER TO A STEP PRESSURE INPUT

Unclassified

Security Classification

DOCUMENT CONTROL DATA - R & D

(Security classification of title, body of abstract and indexing annotation must be entered when the overall report is classified)

1. ORIGINATING ACTIVITY (Corporate author)

Cornell Aeronautical Laboratory, Inc.
Buffalo, New York

2a. REPORT SECURITY CLASSIFICATION

Unclassified

2b. GROUP

-

3. REPORT TITLE

AN EXPERIMENTAL INVESTIGATION OF THE EFFECTS OF A BLAST
WAVE ON A VEHICLE IN A SUPERSONIC FLOW

4. DESCRIPTIVE NOTES (Type of report and inclusive dates)

Task Report

5. AUTHOR(S) (First name, middle initial, last name)

R. Paul Mason

6. REPORT DATE

September 1969

7a. TOTAL NO. OF PAGES

78

7b. NO. OF REFS

15

8a. CONTRACT OR GRANT NO.

N00178-68-C-0313

9a. ORIGINATOR'S REPORT NUMBER(S)

CAL Report No. GM-2673-D-4

b. PROJECT NO.

c.

9b. OTHER REPORT NO(S) (Any other numbers that may be assigned this report)

DISTRIBUTION STATEMENT

Each transmittal of this document outside the Department of Defense
must have prior approval of the Technical Library, U. S. Naval
Weapons Laboratory, Dahlgren, Virginia 22448.

11. SUPPLEMENTARY NOTES

United States Naval Weapons Laboratory
Dahlgren, Virginia 22448 Code GA

13. ABSTRACT

(M equals approximately 2).

A test was conducted to determine the effects of a blast wave on a delta-wing model in a supersonic flow (M=2). Pressure data were taken at various locations on the model using fast-response pressure transducers.

The blast wave was generated by the detonation of a small explosive charge at the apex of a hollow cone normal to the flow direction. The variables of the test were model attitude relative to the charge and simulated altitude.

This report presents details of the facility, blast generator and model, describes the development of instrumentation, and presents the results of the tests.

DD FORM 1 NOV 65 1473

Unclassified

Security Classification

KEY WORDS

LINK A

LINK ■

LINK C

HOLE

W T

ROLE

WT

NOLE

WT